NAVAL POSTGRADUATE SCHOOL

MONTEREY, CALIFORNIA

DISSERTATION

ASSESSMENT OF THE PERFORMANCE OF THE NEAR-BOTTOM HYDROPHONES OF THE U.S. NAVY SOUTHERN CALIFORNIA OFFSHORE RANGE IN DETECTING, LOCALIZING AND RECONSTRUCTING 10-20 KHZ ODONTOCETE WHISTLES

by

Carl Allen Hager

March 2008

Dissertation Supervisor: Ching-Sang Chiu

Approved for public release; distribution is unlimited

THIS PAGE INTENTIONALLY LEFT BLANK

REPORT DOCUMENTATION PAGE			Form Approved OMB No. 0704-0188
Public reporting burden for this collection of information is estimated to average 1 hour per response, including the time for reviewing instruction, searching existing data sources, gathering and maintaining the data needed, and completing and reviewing the collection of information. Send comments regarding this burden estimate or any other aspect of this collection of information, including suggestions for reducing this burden, to Washington headquarters Services, Directorate for Information Operations and Reports, 1215 Jefferson Davis Highway, Suite 1204, Arlington, VA 22202-4302, and to the Office of Management and Budget, Paperwork Reduction Project (0704-0188) Washington DC 20503.			
1. AGENCY USE ONLY ***(Leave blank)***	**2. REPORT DATE** March 2008	**3. REPORT TYPE AND DATES COVERED** Dissertation	
4. TITLE AND SUBTITLE: Assessment of the Performance of the Near-Bottom Hydrophones of the U.S. Navy Southern California Offshore Range in Detecting, Localizing and Reconstructing 10-20 kHz Odontocete Whistles			**5. FUNDING NUMBERS**
6. AUTHOR(S) Carl Allen Hager			
7. PERFORMING ORGANIZATION NAME(S) AND ADDRESS(ES) Naval Postgraduate School Monterey, CA 93943-5000			**8. PERFORMING ORGANIZATION REPORT NUMBER**
9. SPONSORING / MONITORING AGENCY NAME(S) AND ADDRESS(ES) Chief of Naval Operations Environmental Readiness Division (CNO-N45)			**10. SPONSORING / MONITORING AGENCY REPORT NUMBER**
11. SUPPLEMENTARY NOTES The views expressed in this thesis are those of the author and do not reflect the official policy or position of the Department of Defense or the U.S. Government.			
12a. DISTRIBUTION / AVAILABILITY STATEMENT Approved for public release; distribution is unlimited			**12b. DISTRIBUTION CODE**

13. ABSTRACT (maximum 200 words)

A series of 10 to 20 kHz, frequency-sweeping signals synthesizing whistles of vocalizing Odontocetes was transmitted from a J-9 sound projector suspended from the *Research Vessel Pt Sur* while over the U.S. Navy Southern California Offshore Range (SCORE) Underwater Acoustic Range from 11 to 13 August 2004. The transmissions were recorded by a group of seven near-bottom hydrophones of the Range. Using statistical analysis on ensembles of the repeated transmissions, the relationship between probability of detection p(D), probability of false alarm p(FA), signal-to-noise ratio (SNR) of the band-passed hydrophone data and detection range were derived for both a correlator and energy detector. To extrapolate the detection range for a different SL, a ray propagation model was employed. Additionally, the feasibility of using the near-bottom hydrophones of the Range for three-dimensional localization and for reconstructing the source signal waveform was assessed. While the experimental results show that accurate horizontal location estimates can be easily obtained through a minimization of the misfit between the observed and predicted differences in the signal arrival times at a cluster of hydrophones, a high-quality depth estimate is more difficult to accomplish. In order to choose a satisfactory depth estimator, simulated data were used to systematically quantify the sensitivity of the source depth estimates, produced by a set of commonly used frequency and time-domain processing methods to additive noise, sound-speed profile mismatch and hydrophone position errors. The simulation results suggest that a time-domain signal magnitude matching scheme consistently outperforms the other methods. The performance of this scheme was further demonstrated with experimental data. For source signal waveform reconstruction, the sensitivity of a frequency-uncorrelated, least-squares technique to the same errors was investigated.

14. SUBJECT TERMS Matched Field Processing, Odontocete, Magnitude Matching, Time Domain, Localization, Depth Estimation, Acoustic Model, Bottom Hydrophone, Least Squares Estimation			**15. NUMBER OF PAGES** 81
			16. PRICE CODE
17. SECURITY CLASSIFICATION OF REPORT Unclassified	**18. SECURITY CLASSIFICATION OF THIS PAGE** Unclassified	**19. SECURITY CLASSIFICATION OF ABSTRACT** Unclassified	**20. LIMITATION OF ABSTRACT** UU

NSN 7540-01-280-5500 Standard Form 298 (Rev. 2-89)
Prescribed by ANSI Std. 239-18

THIS PAGE INTENTIONALLY LEFT BLANK

Approved for public release; distribution is unlimited

ASSESSMENT OF THE PERFORMANCE OF THE NEAR-BOTTOM HYDROPHONES OF THE U.S. NAVY SOUTHERN CALIFORNIA OFFSHORE RANGE IN DETECTING, LOCALIZING AND RECONSTRUCTING 10-20 KHZ ODONTOCETE WHISTLES

Carl Allen Hager
Commander, United States Navy
B.S., United States Naval Academy, 1986
M.S., Naval Postgraduate School, 1997

Submitted in partial fulfillment of the
requirements for the degree of

DOCTOR OF PHILOSOPHY IN PHYSICAL OCEANOGRAPHY

from the

NAVAL POSTGRADUATE SCHOOL
March 2008

Author: _____
Carl Allen Hager

Approved by:

_____
Ching-Sang Chiu
Professor
Department of Oceanography
Dissertation Committee Chair

_____
Curtis Collins
Professor
Department of Oceanography

_____
Lawrence Ziomek
Professor
Department of Electrical and
Computer Engineering

_____
D. Benjamin Reeder
Research Assistant Professor
Department of Oceanography

_____
James Harvey
Professor
Moss Landing Marine Laboratories

Approved by: _____
Mary Batteen, Professor and Chair, Department of Oceanography

Approved by: _____
Julie Filizetti, Associate Provost for Academic Affairs

THIS PAGE INTENTIONALLY LEFT BLANK

ABSTRACT

A series of 10 to 20 kHz, frequency-sweeping signals synthesizing whistles of vocalizing Odontocetes was transmitted from a J-9 sound projector suspended from the *Research Vessel Pt Sur* while over the U.S. Navy Southern California Offshore Range (SCORE) Underwater Acoustic Range from 11 to 13 August 2004. The transmissions were recorded by a group of seven near-bottom hydrophones of the Range. Using statistical analysis on ensembles of the repeated transmissions, the relationship between probability of detection p(D), probability of false alarm p(FA), signal-to-noise ratio (SNR) of the band-passed hydrophone data and detection range were derived for both a correlator and energy detector. To extrapolate the detection range for a different SL, a ray propagation model was employed. Additionally, the feasibility of using the near-bottom hydrophones of the Range for three-dimensional localization and for reconstructing the source signal waveform was assessed. While the experimental results show that accurate horizontal location estimates can be easily obtained through a minimization of the misfit between the observed and predicted differences in the signal arrival times at a cluster of hydrophones, a high-quality depth estimate is more difficult to accomplish. In order to choose a satisfactory depth estimator, simulated data were used to systematically quantify the sensitivity of the source depth estimates, produced by a set of commonly used frequency and time-domain processing methods to additive noise, sound-speed profile mismatch and hydrophone position errors. The simulation results suggest that a time-domain signal magnitude matching scheme consistently outperforms the other methods. The performance of this scheme was further demonstrated with experimental data. For source signal waveform reconstruction, the sensitivity of a frequency-uncorrelated, least-squares technique to the same errors was investigated.

THIS PAGE INTENTIONALLY LEFT BLANK

TABLE OF CONTENTS

LIST OF FIGURES

THIS PAGE INTENTIONALLY LEFT BLANK

LIST OF TABLES

THIS PAGE INTENTIONALLY LEFT BLANK

ACKNOWLEDGMENTS

I owe an overwhelming ‘thank you’ to many colleagues, advisors, friends and family. In the light of the many circumstances that I have endured over the last four years, this group has not only guided me to completion of this project, but also exemplified / demonstrated the core principles of friendship, commitment, loyalty and perseverance. I owe them more than I will ever be able to express.

First and foremost, I need to thank Dr. Ching-Sang Chiu for his unprecedented guidance and brilliant supervision. His direction was true, direct and expert – the type of no-nonsense mentorship that I needed the most. The remaining - To Dr. Curt Collins, who secured funding for my project and provided countless hours of professional and personal advice, your patience was overwhelming. To Dr. Lawrence Ziomek, Dr. James Harvey and CDR Ben Reeder, USN, Ph.D – for their patience and expertise as committee members; To Chris Miller, M.S., - for exceptional friendship, brilliant and patience assistance, and the formulation of this project. To CDR (ret) John Joseph, USN, for gracious assistance in closing this project out. To Dr. Mary Batteen – for superb patience and mentorship - who has continually been a strong supporter.

I owe considerable thanks to my colleagues at the Naval Academy, who single-handedly pulled me out of a major crisis: To Dr. David Smith for his professional and personal guidance and unquestioned friendship and loyalty. To CDR (ret) Henry Jones, USN, Captain Kathy Shanebrook, USN, Captain Jesse Carman, USN, and Deans William Miller and Michael Halbig for steadfast support and guidance, and also to my fellow faculty members for their patience and flexibility.

A final collective ‘thank you’ to my family and friends: To my Mother, brothers David, Brad and Nelson, and sisters Sue and Mary. I could not have made it through the last 24 months without you. To my dear friends, Patrick Curtin, Lindy Coltharp, Renee Lueck, Rev. David Green, and Larry and Lane Hayes. To Michelle Cox – thank you for accepting my offer for a drink that afternoon in June. I look forward to our future together. And most importantly, to my children Catherine and Jacob – I will always owe

you both a wealth of gratitude for your patience, understanding, and flexibility. You are and will remain my utmost priority. I will always be there for you.

This work was supported by the Chief of Naval Operations Environmental Readiness Division (CNO N45). The author thanks Dr. Ching-Sang Chiu, Dr. Curt Collins, Dr. Lawrence Ziomek, Dr. Ben Reeder, Dr. James Harvey, Mr. Chris Miller and the referees for exceptional guidance and helpful comments.

I. INTRODUCTION

The Navy requires an accurate and robust acoustic detection, localization and classification system to prevent inadvertent exposure of anthropogenic noise to marine mammals, including Odontocetes or "toothed" whales. Although visual surveys provide a basis for avoidance, this method is not continuously employed during military operations and unfeasible at night and in fog and bad weather. Acoustic detection methods appear very promising, but for Odontocetes, specific challenges include high transmission losses (surface and bottom roughness scattering and chemical relaxation), significant variability inherent with calls, and identification of specific species in the cacophony of high density, multiple animal vocalizations.

Odontocete vocalizations can generally be categorized into two types, clicks and whistles. The focus of this dissertation is on the whistles, which typically have lower source levels, smaller bandwidths, longer durations and lower upper frequency bounds. Designed originally to track torpedoes and submarines during military exercises, the Southern California Offshore Range (SCORE) hydrophone array has exceptional potential for tracking and localizing these whistles, specifically those that sweep within or through the designed bandwidth (~ 8-40 kHz). Digital recordings from seven hydrophones of this array collected during a playback experiment were used as data for this study.

This dissertation, funded by the Chief of Naval Operations Environmental Readiness Division (CNO-N45) and supported by the Naval Postgraduate School Ocean Acoustics Laboratory, consists of two papers for submission to the Journal of the Acoustical Society of America. The objective of the first paper (Section II) entitled "Assessment of Detection Performance of the near-bottom Hydrophones at the U. S. Navy SCORE Underwater Acoustics Range using a playback of Representative Odontocete Vocalizations," is to quantify the performance of the near-bottom hydrophones in detecting Odontocete vocalizations. The objective of the second paper (Section III), entitled "Three Dimensional Localization and Source Signal Waveform Reconstruction of Representative Odontocete Vocalizations at the U.S. Navy SCORE

Underwater Acoustic Range," is to assess the feasibility of using the hydrophones for three-dimensional localization and for reconstructing the source signal waveform.

The first paper represents an extension of the work by Garcia (2002) and Daziens (2004) who investigated the performance statistics and detection ranges of mid-frequency (1-8 kHz) Odontocete whistles using hydrophones moored or tethered at mid or upper depths of the water column. Data was collected during a playback experiment. A similar approach was adopted here, although this study will utilize a very different receiver system with near-bottom hydrophones monitoring at a different frequency band. The approach entailed carrying out a playback experiment at the SCORE Range followed by analysis of the statistics of the output of energy and correlator detectors. The output statistics of these two detectors were investigated because they represent the lower and upper performance bounds, respectively. Additionally, in order to extrapolate the detection range for a different SL, a ray propagation model was employed.

The horizontal localization portion of the second paper is similar to a model-based approach used by Tiemann *et al.* (2002), who achieved horizontal localization of vocalizing Humpback whales through a minimization of the misfit between the observed and predicted differences in the signal arrival times at an U.S. Navy Underwater Acoustic Range in Hawaii. The depth estimation and source signal reconstruction portion is similar to previous work done by Moore (1999) and Chiu *et al*. (2003). Moore achieved a localization of a vocalizing blue whale via matched signal processing (MSP) as well as retrieval of the source signature via least-squares fitting of modeled waveforms to received data. Moore and Chiu conducted MSP of vocalizations at approximately 50 – 90 Hz. This study will focus on a much higher frequency regime (~10-20 kHz).

The uniqueness of the second paper involves the extensive computer simulation undertaken to quantify the localization performance of commonly used frequency and time-domain processing methods when faced with additive noise, environmental mismatch and hydrophone positional error. The results of these sensitivity studies, supplemented with experimental playback results, allows for the selection of an estimator of choice at the Range. Additionally, for source waveform reconstruction, the sensitivity of a frequency-uncorrelated, least-squares technique to these errors will be investigated.

II. ASSESSMENT OF DETECTION PERFORMANCE OF THE NEAR-BOTTOM HYDROPHONES AT THE U. S. NAVY SCORE UNDERWATER ACOUSTIC RANGE USING A PLAYBACK OF REPRESENTATIVE ODONTOCETE VOCALIZATIONS[1]

A. ABSTRACT

A series of synthesized whistle signals of vocalizing Odontocetes was transmitted from a J-9 sound projector suspended from the *Research Vessel Pt Sur* while over the U.S. Navy SCORE Underwater Acoustic Range from 11 to 13 August 2004. The transmissions were recorded by a group of seven near-bottom hydrophones of the Range. Using statistical analysis on ensembles of the repeated transmissions, the relationship between probability of detection p(D), probability of false alarm p(FA) and signal-to-noise ratio (SNR) of the band-passed hydrophone data and detection range were derived for both a correlation detector (correlator) and energy detector. Specifically, the empirical relations show: (1) For a source level (SL) of 135 dB re 1 μPa , p(D) of 95% , and p(FA) of 0.01%, the corresponding detection ranges for a 1 s long, 20 – 10 kHz downsweep chirp are 1600 m for the energy detector and 5100 m for the correlator in the presence of clutter, i.e., actual Odontocete calls with roughly similar signal characteristics as the synthesized calls. (2) In the absence of clutter, the detection range for the energy detector increases to 2400 m, while the performance for the correlator remains unchanged. (3) To achieve the 95% p(D) and 0.01% p(FA), the energy detector requires a SNR of -2.2 dB and -5.3 dB in the presence and absence of clutter, respectively. To extrapolate the detection range for a different SL, a ray propagation model was employed. The modeled transmission loss (TL) shows a 600 m increase in the detection range for each 3 dB increase in SL. Maintaining -5.3 dB as the required SNR, an application of this model projection over the area surrounded by the seven hydrophones shows a 100% detection area coverage when SL reaches 138 dB re 1 μPa.

1This chapter is formatted for submission to the Journal of the Acoustical Society of America.

B. INTRODUCTION

Anthropogenic noise, including Navy sonar operations, poses a threat to existing marine mammal populations. Berggren *et al*. (2002), Clark (1994/1995), Croll *et al.* (2001), Frankel and Clark (1998/2000), and Moore and Clark (2002), are examples of recent and continuing studies of anthropogenic effects on marine mammals. In the interest of quantifying these effects, extensive behavioral response studies following exposure to both high and low frequency noise have been conducted by Schlundt *et al*. (1999), Nachtigall *et al*. (2003), Finneran *et al*. (2002), and Au *et al*. (1997).

The Navy requires an accurate and robust acoustic detection, localization and classification system to prevent inadvertent exposure of anthropogenic noise to marine mammals, including Odontocetes or "toothed" whales. Although visual surveys provide a basis for avoidance, this method is not continuously employed during military operations and is unfeasible at night or in fog or severe weather. Acoustic detection methods appear very promising, but for Odontocetes, specific challenges include high transmission losses (surface and bottom roughness scattering and chemical relaxation), significant variability inherent with Odontocete calls, and identification of specific species in the cacophony of high density, multiple animal vocalizations.

One of the first concentrated research projects involving the detection and localization of marine mammals utilized the Navy's recently unclassified SOSUS (Sound Underwater Surveillance System) hydrophone array. Designed originally to track Cold War submarines, this fixed surveillance system immediately emerged as an excellent large area, passive sensor to monitor the low frequency vocalizations of Mysticetes or "Baleen" whales. SOSUS monitor, tracking, detection performance, and census studies for Mysticetes have been conducted by Chiu *et al*. (1999/2003), Clark *et al*. (1994/1995/1998), Hager (1997), Kumar *et al*. (2002), Moore (1999), and Nishimura *et al*. (1994) among others.

Examples of Odontocete vocalizations include high frequency echolocation "clicks" and frequency-modulated "whistles" described in Herman and Tavolga (1980), Au (1993), and Richardson *et al*. (1995). Clicks are broadband, short duration, and

relatively high power spectrum source level (>200 dB re 1 $\mu Pa^2 / Hz$) vocalizations used for echolocation and are described in Rasmussen *et al*. (2002), Mohl *et al*. (2000/2003), Thode *et al*. (2002), Madsen *et al*. (2003), Au and Herzing (2003), Au *et al*. (2004), Philips *et al*. (2003), and Frantzis *et al*. (2002). Whistle source levels are significantly lower, varying from approximately 120 to 160 dB re 1 μPa @ 1m as described in Watkins and Scheivll (1974), Janik *et al*. (2000), and Thomsen *et al*. (2001). Whistles have been successfully localized and tracked using a three-element hydrophone towed array (Thode, 2000), a sonobuoy array (Howarth, 2003), and through frequency domain beamforming using a narrow aperture audio/video array. (Ball and Buck, 2003) Frietag and Tyack conducted passive acoustic localization of whistles as well (Frietag and Tyack, 1993).

C. OBJECTIVES / APPROACH

The objective of this study is to quantify the performance of the near-bottom hydrophones of the SCORE Underwater Acoustic Range in detecting Odontocete vocalizations. These vocalizations can generally be categorized into two types, clicks and whistles. The focus of this performance study is on the whistles, which typically have lower source levels, smaller bandwidths, longer durations and lower upper frequency bounds. Designed originally to track torpedoes and submarines during military exercises, the SCORE hydrophone array has exceptional potential for tracking and localizing those whistles that sweep within or through the designed bandwidth (~ 8-40 kHz) of the SCORE array.

This study represents an extension of the work by Garcia (2002) and Daziens (2004) who investigated the performance statistics and detection ranges of mid-frequency (1-8 kHz) Odontocete whistles using hydrophones moored or tethered at mid or upper depths of the water column. Data was collected during a playback experiment. A similar approach is adopted here. This study will utilize a very different receiver system with near-bottom hydrophones monitoring at a different frequency band. The approach entailed carrying out a playback experiment at the SCORE Range followed by analysis of

the statistics of the output of energy and correlation detectors. The output statistics of these two detectors were investigated because they represent the lower and upper performance bounds, respectively.

The playback experiment transmitted a train of representative Odontocete (10-20-kHz) whistles using a J-9 sound source deployed from a research vessel to a depth of approximately 15 m. The same series of transmissions were repeated at each of seven equally spaced stations forming a linear track inside an area spanned by a hexagonal sub-array consisting of seven near-bottom hydrophones. The playback experiment, including the geometry and the signaling and recording schemes are detailed in Sec. D. Chi-square distributions were then fitted to empirically derived histograms of the detector output peaks for the different propagation ranges in the presence and absence of the transmitted signal. This allowed for calculation of the SNR-dependent (or range-dependent) relation between p(D) and p(FA). The choice of p(D) and p(FA) values then provides an estimate of the required SNR or detection range for the SL used. The formula for the detectors and the analyzed results of the output statistics are presented in Sec. E. Given that the experimental SL was limited to 135 dB re 1 μPa, it would be useful to extrapolate the empirical results to a higher SL. The extrapolation was accomplished using a ray-theory based, multipath transmission loss (TL) model. This TL model and the predicted dependence of detection coverage on SL are discussed in Sec. F. Major conclusions of this study are provided in Sec. G.

D. DATA COLLECTION

1. SCORE Range Bathymetry and Near-Bottom Hydrophone Distribution

The *Research Vessel Point Sur*, based out of Moss Landing, California and contracted through the Moss Landing Marine Laboratories, provided the research platform for this experiment. The experiment was conducted from 11 to 13 August 2004 at the SCORE Underwater Acoustic Range. The Range is located on the western side of San Clemente Island. The carpeted array covers a natural "bathtub" contour. The extremes of the depths at the Range vary from 1700 m in the northwest to 700 m in the southeast. The portion of the array utilized for this experiment, displayed in Figure 1,

includes hydrophones numbered 55, 61, 69, 70, 71, 77 and 78 which form a hexagon array with Hydrophone 70 in the middle location. The hydrophones in this subset array occupy depths from 1000 to 1300 m.

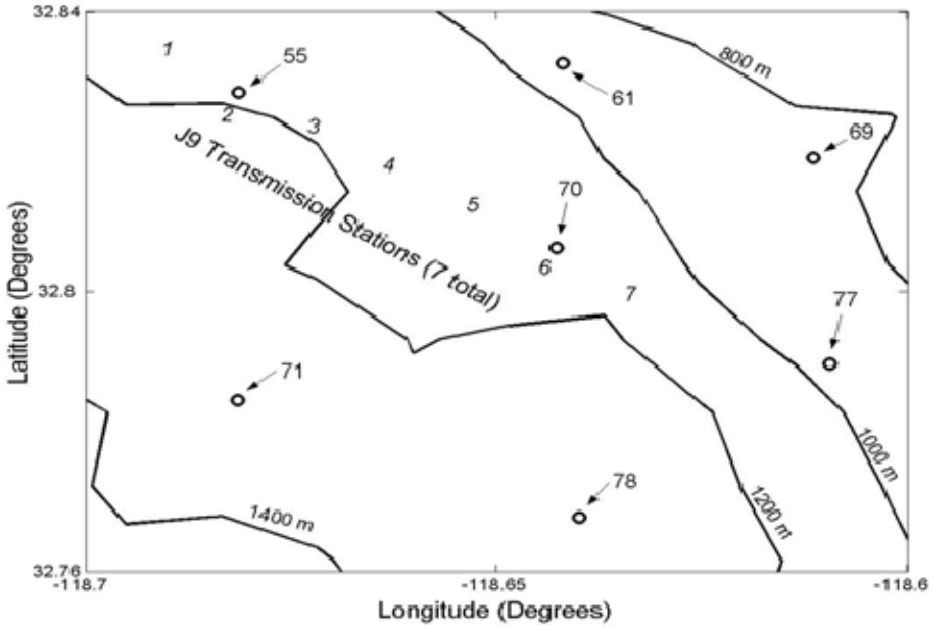

Figure 1. Geometry of the playback experiment showing locations of the seven transmission stations and nearby hydrophones. The bathymetry is also shown by isobaths using a 200 m contour interval.

2. Experiment Description

a. J-9 Sound Source Transmission

Upon entering the range at approximately 2330 (L) on 11 August, the *RV Pt Sur* positioned over Hydrophone 55 and began a succession of transmission stations equally spaced at 1000 m and along a straight line (Stations 1 – 7) utilizing a J-9 sound projector at 15 m depth. Station 1 recordings were not utilized in the detection performance study. Station 2 represented the closest distance (directly overhead) to Hydrophone 55 and Station 7 represented the farthest. Figure 1 details the geographic progression of the transmission stations.

Ten and twenty kHz was the lower and upper bounds of the transmission signal bandwidth. Several Odontocete species whistle within this bandwidth. Bazura-

Duran and Au (2002) detailed six general categories of Spinner Dolphin whistle contours. Three of these contour shapes were synthesized for this study. The transmitted signal consisted of a one-second, 10-20 kHz linear sweep, a three-second, "concave" whistle, a one-second, 20 to 10 kHz "down-sweep" whistle, and a 10 to 15 kHz "upsweep" whistle. With three second gaps between each whistle, the transmission sequence was approximately 15 s in duration (Figure 2). The sequence was transmitted 78 times at each station.

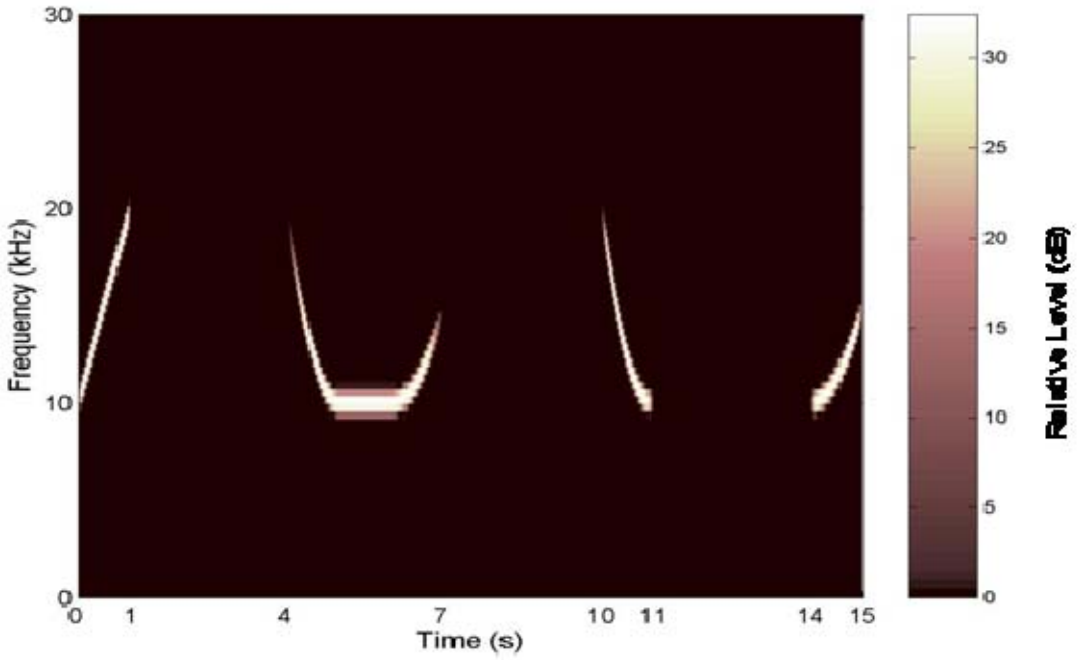

Figure 2. The spectrogram of the signal transmitted by the J-9 sound source. The sequence consisted of a 1 s, linear frequency-modulated (FM) "up-sweep" and a succession of contoured, FM whistles. The whistle transmitted at 10 -11 s into the sequence was utilized in this study. The additional contours are designed for future work

b. Source Level Calculation

In order to measure the mean-squared pressure at 1 m distance from the J-9 sound projector, a monitoring hydrophone and associated cabling was attached to the cable for the J-9 so as to hang 1 m below the source. At 15 m of source depth, the monitoring hydrophone was at a depth of 16 m. The hydrophone sensitivity, -164 dB re 1V/μPa, was applied to the voltage time series $v_o(t)$, was done to obtain the pressure oscillation time series, $p_0(t)$ in μPa. Source level (SL) was then calculated as:

$$SL = 20\log_{10}\left[\frac{\sqrt{\frac{1}{T}\int_0^T p_o^{\,2}(t)dt}}{1\mu Pa}\right] dB \ , \qquad (1)$$

where T is the duration (1 s) of the downsweep whistle. SL was estimated to be 135 dB re 1 μPa @ 1m .

c. Hydrophone Data Collection

Two portable shipboard computer rack systems were utilized. The first rack system consisted of a personal computer (PC), a PC sound card, amplifier, and cabling to the J-9 projector lowered to a depth of 15 m. Data for the bottom mounted hydrophones was recorded at the San Clemente Island cable termination van at an 80 kHz sampling rate. Data was saved in 5 minute "packets" of approximately 750 megabytes onto a single hard drive.

3. Experimental Issues

Two issues were identified during the course of this experiment that merit discussion. They are the effects of background noise (platform noise and actual marine mammal vocalizations) on detection performance analysis and the Automatic Gain Control (AGC) for the bottom hydrophones. The bottom hydrophones have a hard-wired or fixed AGC that decreases amplitude when the received levels are too high. Because of AGC adjustments and lack of "end-of-cable" sensitivity, conversion from volts to μPa was not accomplished.

a. "Clutter" or False Detections

When either the correlator or energy detector found an actual Odontocete vocalization rather than an intended playback signal, the output was designated as "clutter". Although the energy detector experienced more clutter, a closer analysis of spectrograms associated with bottom hydrophone digital recordings revealed that individual animals engaged in interrogation and response dialogues with the J-9. This also produced correlator clutter. A mimicking of the signal by nearby animals was widespread throughout the recordings.

b. Automatic Gain Control (AGC)

Figure 3 depicts an AGC adjustment affecting the recorded data of the transmitted downsweep on Hydrophone 70. A step up and a step down are evident. Although Hydrophone 70 had a significant AGC control, three additional hydrophones that detected this upsweep did not appear to be affected by AGC. Hydrophone 70 was the closest to the source at transmission for this recording.

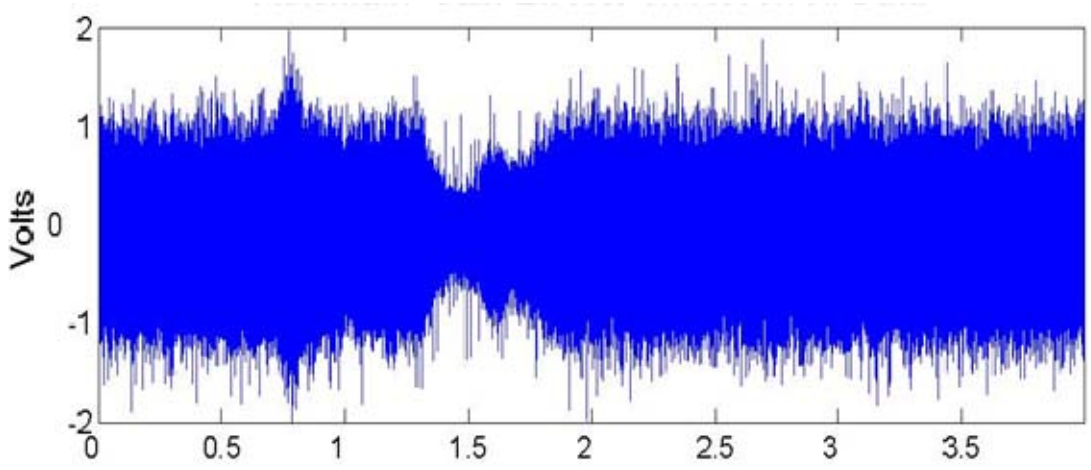

Figure 3. Automatic Gain Control (AGC) effects on recorded hydrophone voltage amplitude during a "loud" event. The spike at .8 s represents the start of the FM downsweep. The signal's duration is 1 s.

E. EXPERIMENTAL DETECTION PERFORMANCE EVALUATION

1. Formulation

a. Histograms of Peak Detector Output

Two detection schemes were utilized in this study. The "energy detector" is an incoherent detector and exploits a signal's energy content. It is indiscriminative to the characteristics of a waveform, but suffers a lower processing gain (Urick, 1983). The"correlator" is a coherent detector and requires prior knowledge of a transmitted waveform's characteristics. The correlator's success is based upon the prior construction of a "replica" signal.

Data, *r(t)*, was digitized at a sampling rate of 80 kHz and band-pass filtered for noise reduction. The "replica" source signal waveform, *s(t)*, was correlated with *r(t)* as

$$c_{COR}(\tau) = \sum_{n=1}^{N} s(t_n - \tau) r(t_n) \Delta t , \qquad (2)$$

while a "boxcar," *u(t)*, waveform was correlated with $r^2(t)$ for the energy detector as

$$c_{ED}(\tau) = \sum_{n=1}^{N} u(t_n - \tau) r^2(t_n) \Delta t . \qquad (3)$$

In (2) and (3), Δt = 1/80 kHz and $N\Delta t$ =1 s, the duration of the replica or the boxcar. Both *s(t)* and *u(t)* were normalized to unit energy.

Peak correlator output represents a quantitative measure of the "likeness" of the signal to the replica signal. The peak energy detector output represents a quantitative measure of an event's energy. Correlator and energy detector output hereafter refer to the peak value attained with each method.

Using the entire ensemble of 78 total transmissions of the 1 s down-sweep per station, histograms were constructed of correlator and energy detector output. The station "signal-plus-noise" histograms were constructed of correlator and detector output when the signal was present while the "noise-only" histograms were constructed when

the signal was not present. Energy detector output signal-plus-noise histograms are displayed in blue color and noise-only histograms are displayed in yellow color in Figure 4. Correlator output histograms are not shown.

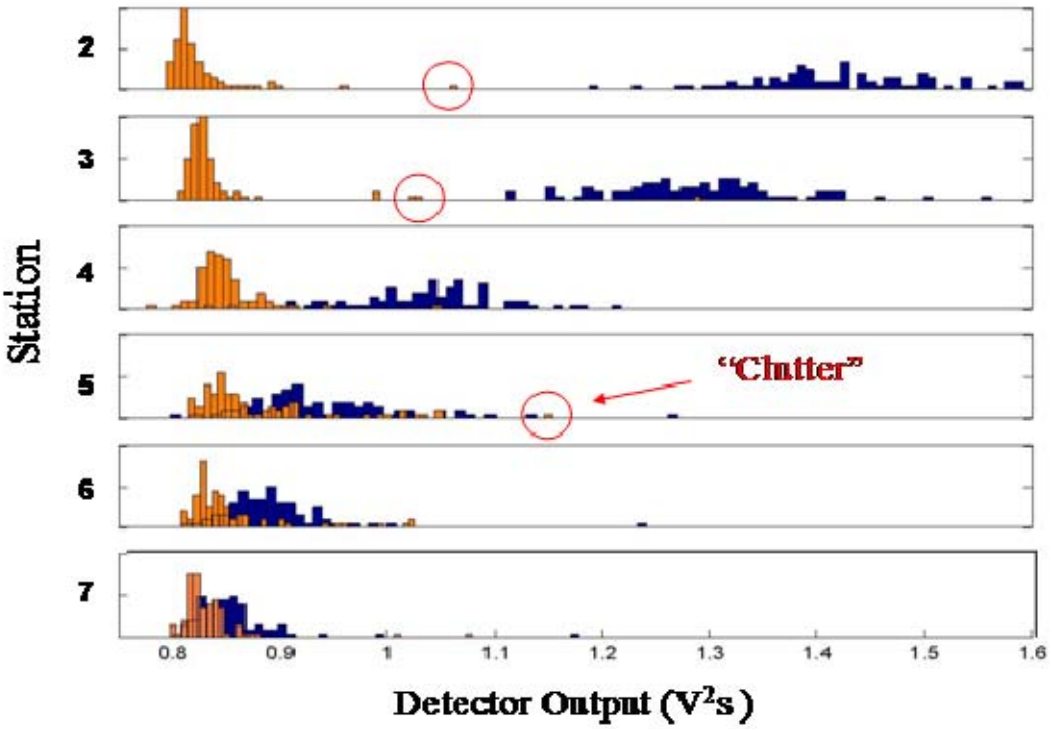

Figure 4. Station signal-plus-noise (blue) and noise-only (yellow) energy detector output histograms for Hydrophone 55. The red circles in this diagram show clutter.

b. Probability Density Function (PDF) Representations of Detector Output

The theoretical consideration for best fitting the empirical histograms to a statistical distribution is based upon a study (Dyer, 1970) of transmission fluctuations in a phase random multipath environment. Dyer found that the density of mean squared pressure adhered to a chi-square (χ^2) distribution with the number of degrees of freedom dependent upon the number of independent events or arrivals. Because the energy detector is subject to a multipath, random phase and amplitude environment, the χ^2

distribution was chosen to "best-fit" the signal-plus-noise and noise-only empirically derived histograms.

Figure 5 reveals the relationship between station signal-plus-noise PDFs and representative noise-only PDFs. Two noise-only PDFs were utilized in this study. The noise-only "clutter present" PDF (lower left in Figure 5) has a larger variance and mean value than the noise-only "clutter absent" PDF (upper right in Figure 5). This figure also reveals that the signal-plus-noise PDFs transition from high to low degrees of freedom as SNR (dB) decreases. Complete overlap of the signal-plus-noise PDF and noise-only PDF represents a SNR (dB) of $-\infty$.

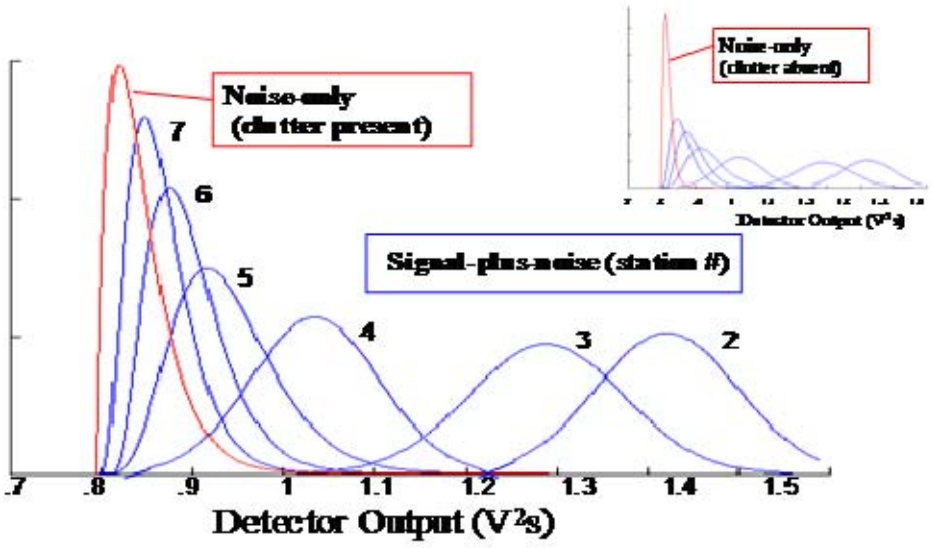

Figure 5. Successive χ^2 signal-plus-noise (blue) and noise-only (red) PDFs that best fit corresponding detector output histograms in the presence of clutter. For comparison, the relationship between signal-plus-noise PDFs and the noise-only PDF without clutter is shown in the upper right.

Functions $f(q)$ and $g(q)$ represent unity area signal-plus-noise and noise-only PDFs respectively. A relationship between p(D) (4) and p(FA) (5) can be established by varying a correlator or energy detector output threshold value, designated "*thr*" , from zero to infinity as

$$p(FA) = \int_{thr}^{\infty} f(q)dq \text{ and } p(D) = \int_{thr}^{\infty} g(q)dq \qquad (4,5)$$

(Urick, 1983).

Each threshold value in turn yields an independent value for both p(D) and p(FA) . The results are then plotted as a Receiver Operating Characteristics (ROC) Curve for each transmission station.

c. Receiver Operating Characteristics (ROC) Curves and Input SNR

The resultant ROC curves for Hydrophone 55 in the presence of clutter are shown in Figure 6. It is important to note that each ROC curve represents both an input SNR and distance from hydrophone to transmitter. For each station, the input SNR was established as

$$\text{SNR} = 10\log_{10}\left[\frac{\mu_{s+n}}{\mu_n} - 1\right] dB, \qquad (6)$$

where "$\boldsymbol{\mu}_{s+n}$" and "$\boldsymbol{\mu}_{n}$" represent the ensemble mean of signal-plus-noise and noise-only energy detector output respectively. For the remainder of this study, SNR will refer to the input SNR calculated by (6).

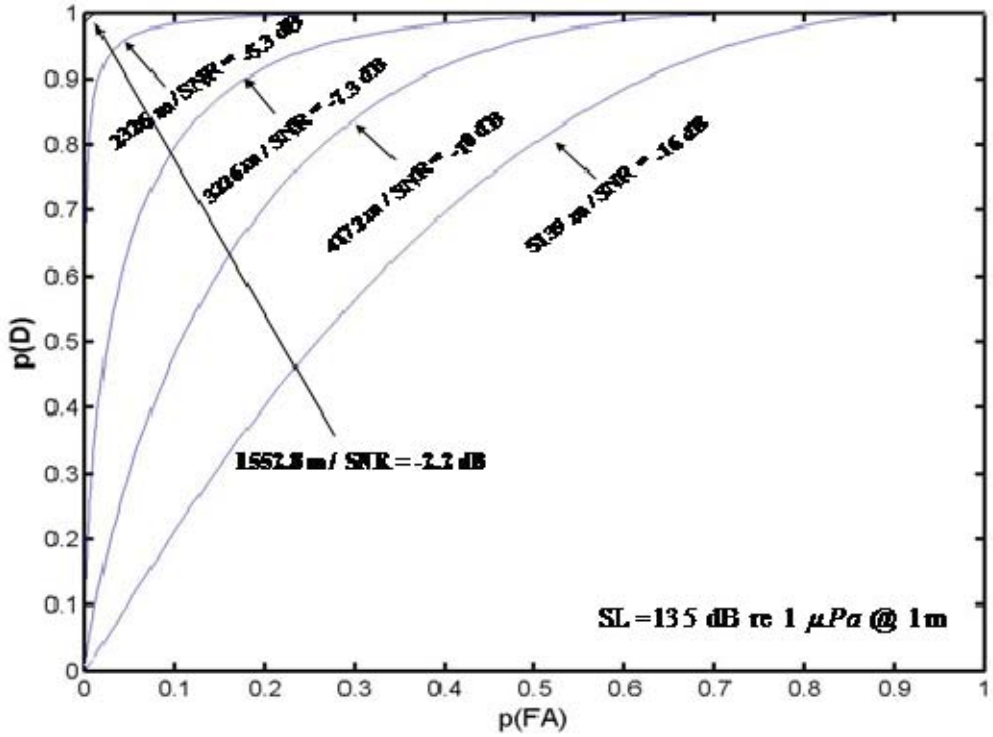

Figure 6. Experimental energy detector output ROC curves calculated from signal-plus-noise and noise-only (clutter present) PDFs for each station. The distance to each station and SNR are given for each curve. The Station 2 curve is not shown due to AGC gain.

2. Experimental Results - p(D) vs. SNR or Detection Range

Figure 7 displays transition curves obtained by applying a fixed false alarm rate to the ROC curves in Figure 6. Constructed from energy detector (in the presence *and* absence of clutter) and correlator ROC curves, the transition curves reveal the detection range or SNR required given selected values of p(D) and p(FA). Detection ranges, obtained from the curves for a p(D) of 95% and p(FA) of .01%, were calculated as 1600 m (energy detector) and 5100 m (correlator) in the presence of clutter. In the absence of clutter, the energy detector detection range increased to 2400 m. Required SNRs for the energy detector under the same constraints were -2.2 dB (clutter) and -5.3 dB (no clutter)

respectively. These detection ranges are associated with a one second, downsweep, FM signal transmitted from 20-10 kHz, with $SL \cong 135\ dB$ re 1 μPa @ 1m.

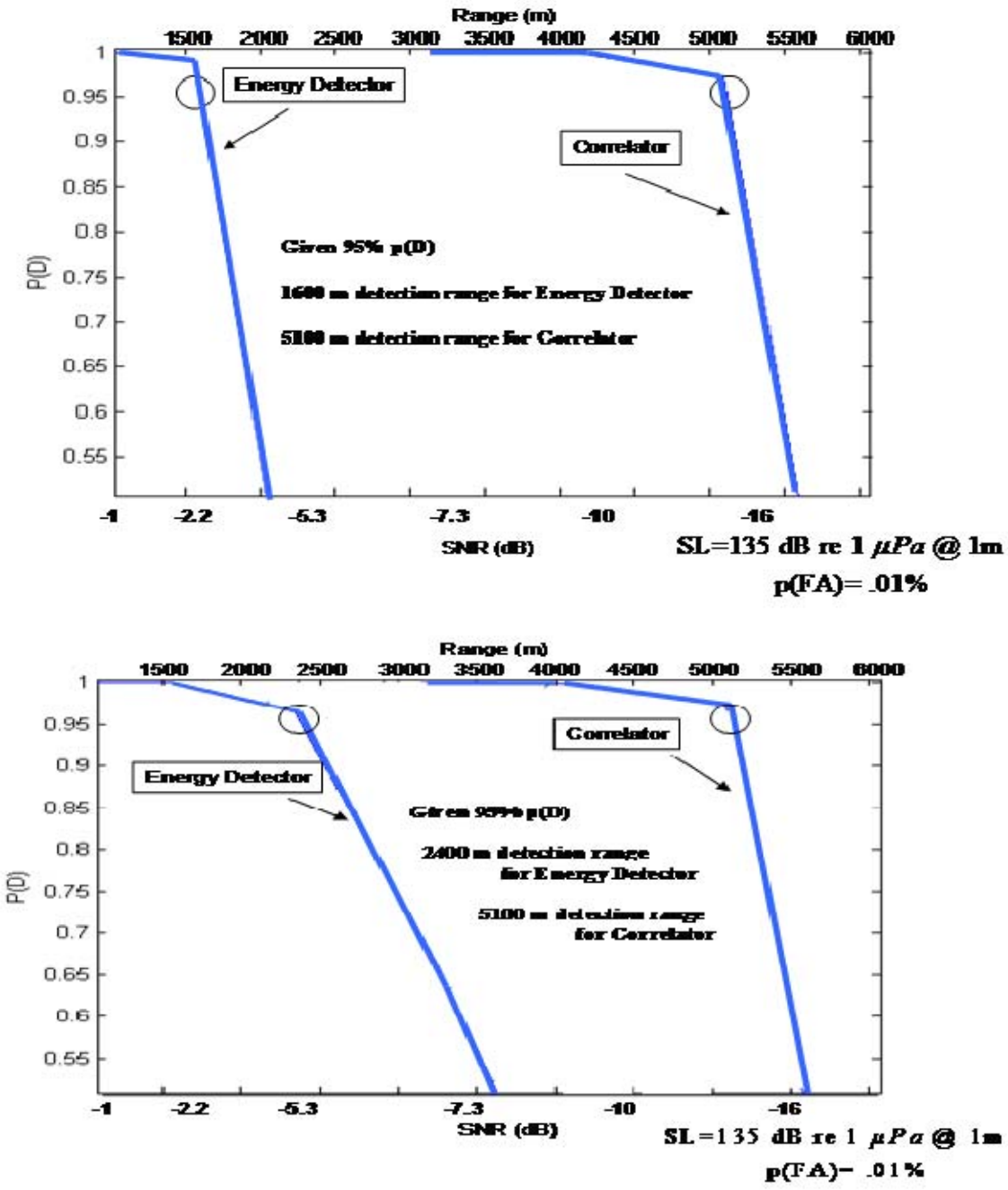

Figure 7. P(D) vs. SNR or detection range transition curves in the presence of clutter (top) and without clutter (bottom) for a fixed p(FA) of .01%. The circles in this figure denote the range where p(D) = 95%.

F. DETECTION RANGE VS SL PREDICTION

It must be noted that the detection range and required SNR obtained in the previous section are for *fixed* values of p(D) at 95%, p(FA) at .01%, and SL of 135 dB re 1 μPa @ 1m. Because the transmitted SL is 5 - 25 dB less than most of the published Odontocete frequency-modulated vocalizations (Watkins and Schevill, 1974, and others), it would be valuable to estimate changes in the detection range in response to elevated source levels. This can be accomplished using modeled transmission loss (TL). A range increase can then be applied to a plan view of all hydrophones in the hexagonal array to visually indicate the increased detection area coverage.

1. Four Ray Path Broadband TL Model

Because the J-9 sound source transmitted at a distance from the hydrophone, the sound arrived at the receiver via an ensemble of possible ray paths. The Hamilton Acoustic Ray-Tracing Program for the Ocean (HARPO) was used to calculate these ray paths. By numerical integration of the Hamilton's Equations, this program traces the paths of acoustic rays were traced as they traveled through an analytic model ocean. The original version of this program (Jones *et al*., 1986) was upgraded in 1994 (Chiu *et al*. 1994) to allow for the input of gridded bathymetry and sound speed data. The upgraded program was used in this study.

Output from the program allowed for identification of the four dominate paths or "eigenrays" shown in Figure 8; the direct path ray, the surface reflected ray, the bottom reflected ray, and the bottom *and* surface reflected ray. Given this output, the eigenray's signal amplitude a_n , phase shift ϕ_n , and travel time t_n, can be computed in order to construct a predicted (superscripted "*m*" for modeled and subscripted "*p*" for the specific hydrophone) transfer function. The transfer function $H_p^m(f)$ is

$$H_p^m(f) = \sum_{n=1}^{4} a_n(f) e^{-i(2\pi f t_n \pm \varphi_n)} \quad , \qquad (7)$$

where the $\pm$ values in the exponential correspond to frequencies greater than and less than zero respectively.

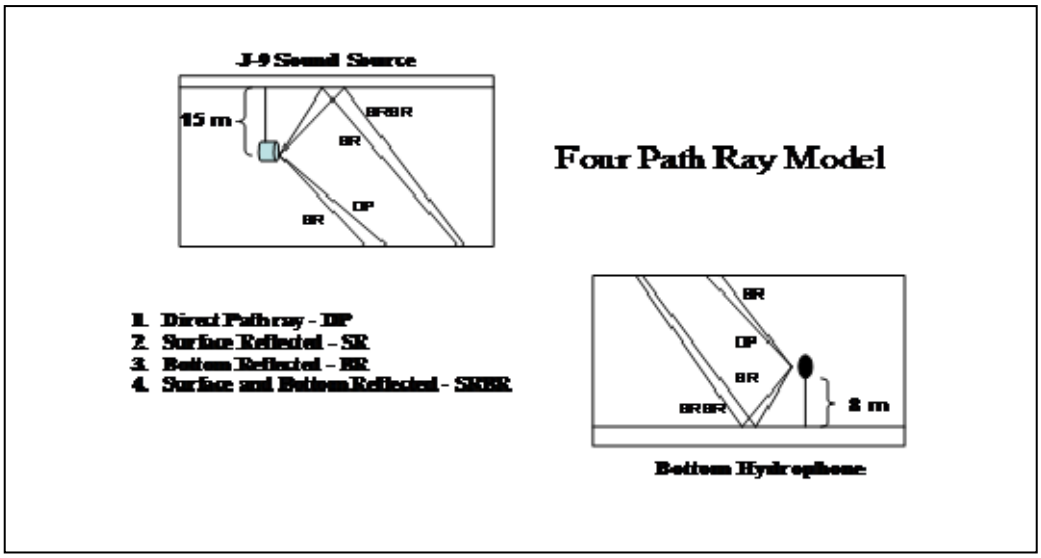

Figure 8. The four rays, consisting of a direct path (DP), surface reflected (SR), bottom reflected (BR), and surface *and* bottom reflected (SRBR), coherently summed to create the predicted arrival voltage time series $r_p^m(t)$ for a single hydrophone.

In (7), both phase, ϕ_n, and travel time, t_n, are independent of frequency. Modeled phase corrections have a negative value and result from surface and bottom reflections. The eigenray amplitude, a_n, accounted for bottom, surface and absorption losses. Bottom and surface reflection losses were calculated as a function of sediment sound speed, density and wave height. Absorption loss was calculated as a function of temperature, salinity, pH, frequency and depth of water column (Urick, 1983). The predicted real signal, $r_p^m(t)$, is then calculated as

$$r_p^m(t) = \int S(f) H_p^m(f) e^{i2\pi ft} df \,, \qquad (8)$$

which is the inverse transform of the source signal spectra multiplied by the spectra of the predicted transfer function. The TL versus range is then calculated as

$$TL(r) = +10\log_{10}\left[\frac{\int s(t)^2 dt}{\int r_p^m(t;r)^2 dt}\right]. \qquad (9)$$

Because TL varies with frequency, i.e. a higher attenuation occurred at 20 kHz than at 10 kHz, the broadband TL calculated in (9) represents a mean value of TL over the band. Results are displayed in Figure 9.

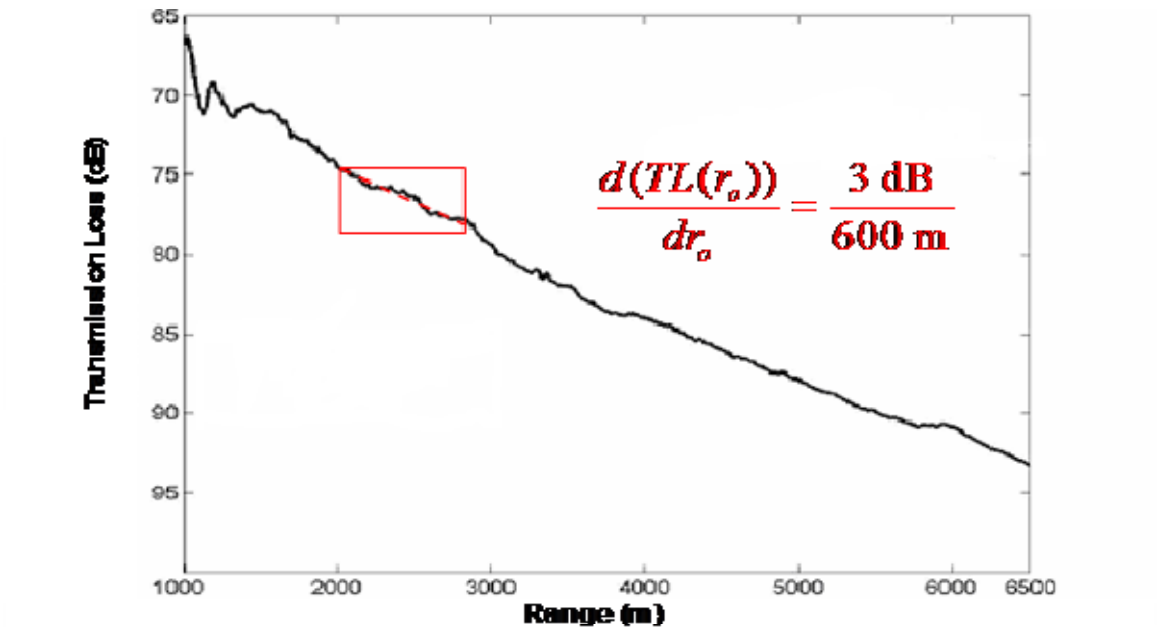

Figure 9. Averaged TL as a function of range from the hydrophone. A relatively constant gradient of 3 dB per 600 m range increase / decrease is shown in the red box.

2. Detection Range and Detection Area Coverage vs. SL

The experimentally obtained SNR required to achieve a 95% p(D) and .01% p(FA) is related to the SL, noise level (NL), and TL as

$$SNR_{required} = SL - TL(r_o) - NL \ , \qquad (10)$$

where r_o represents the detection range. In order to maintain the same required SNR, a change in SL would require a change in r_o . This change in SL with respect to r_0,

$$\frac{d(SL)}{dr_o} = \frac{d(TL(r_o))}{dr_o} \ , \qquad (11)$$

is relatively constant and equal to 600 m per 3 dB change. In other words,

$$\frac{\Delta r_o}{\Delta SL} = \left[\frac{600m}{3dB} \right] . \qquad (12)$$

A 2400 m radius circle (displayed as dashed blue in Figure 10) surrounding a single hydrophone defines a detection area that ensures at least a p(D) of 95% and p(FA) of .01% for a source transmitted at a SL $\cong$135 dB re 1 μPa @ 1m. A 3 dB increase in SL expands each hydrophone detection range by 600 m and expands the area of high probability coverage. Figure 10 shows that the seven hydrophone array would achieve a 95% p(D) and .01% p(FA) on at least one hydrophone of the array if a signal was transmitted with similar characteristics at a SL of 138 dB re 1 μPa @ 1 m anywhere within the field.

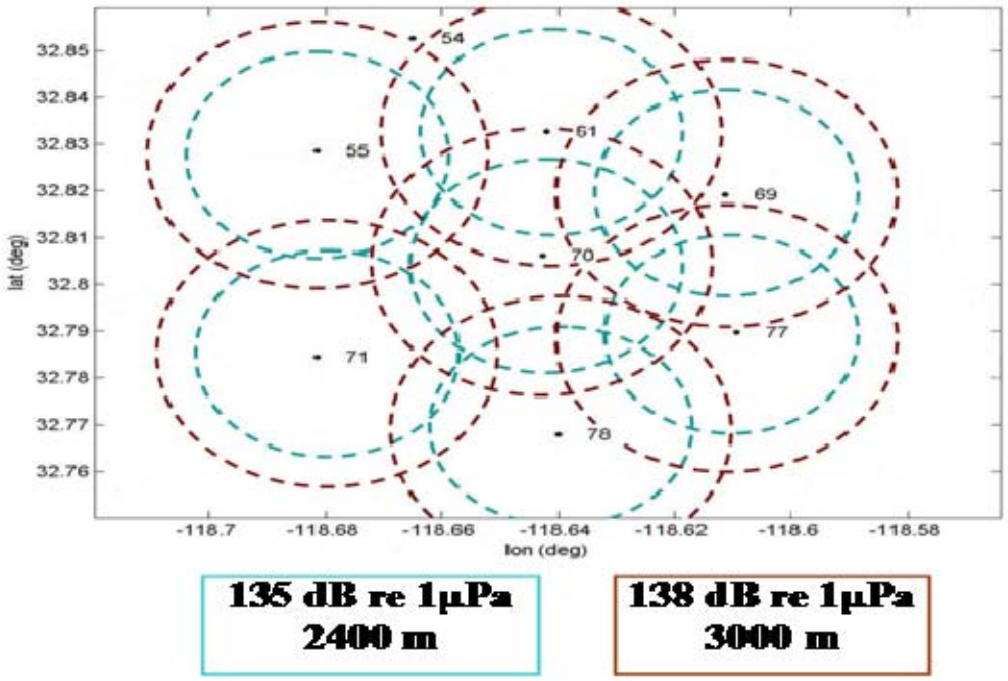

Figure 10. Subset array detection area coverage comparison (assuring a 95% p(D) and .01% p(FA)) for source levels of 135 dB (blue) and 138 dB (red) re 1 µPa.

G. SIGNIFICANT RESULTS / CONCLUSIONS

The objective of this study was to quantify the performance of the near-bottom hydrophones of the SCORE Underwater Acoustic Range in detecting Odontocete vocalizations. The study utilized data (bottom hydrophone recordings of a transmitted synthetic series of Odontocete vocalizations) collected during a "playback" experiment while over the U.S. Navy SCORE underwater acoustic range 11-13 August 2004. Specifically, the signal recorded was a 1 s duration, contoured, FM down-sweep from 20 to 10 kHz transmitted at a SL of 135 dB re 1 μPa @ 1 m. A statistical analysis of ensemble (78 transmissions at each station) recordings of this data resulted in high p(D) (95%) and low p(FA) (.01%) detection range estimates for a correlator and energy detector. It is important to provide a lower and upper bound of expected detection ranges for this type of vocalization. The energy detector provided the lower bound while the correlator provided the upper bound.

Experimentally obtained detection ranges were 1600 m (energy detector) and 5100 m (correlator) in the presence of clutter. In the absence of clutter, the energy detector range increased to 2400 m. Required SNRs for the energy detector ranges were -2.2 and -5.3 dB respectively. This detection range variation reveals the challenge of conducting a playback experiment in the presence of animals engaging in an interrogation / response dialogue with a sound source. The detector output clutter is an unavoidable by-product of the experiment because marine mammal vocalizations were recorded simultaneously with synthetic transmissions. A strong vocalization can trigger a false detection and mask the playback transmission.

Finally, experimentally obtained SNR and detection ranges combined with a four path, broadband TL loss model resulted in detection range predictions for a SL increase. A 600 m range increase per 3 dB SL increase was extracted from a modeled TL curve. Most notably, a 3 dB increase in SL from that transmitted in this study resulted in complete area coverage that assures a p(D) of 95% and p(FA) of .01% for the seven bottom hydrophones that recorded data.

THIS PAGE INTENTIONALLY LEFT BLANK

III. THREE DIMENSIONAL LOCALIZATION AND SOURCE SIGNAL WAVEFORM RECONSTRUCTION OF REPRESENTATIVE ODONTOCETE VOCALIZATIONS AT THE U.S. NAVY SCORE UNDERWATER ACOUSTIC RANGE[2]

A. ABSTRACT

The feasibility of using the near-bottom hydrophones of the U.S. Navy Southern California Offshore Range (SCORE) for three-dimensional localization of frequency-sweeping Odontocete vocalizations in the 10-20 kHz band and for reconstructing the source signal waveform was assessed. For localization, the assessment employed both computer simulated data and actual measurements collected from a "playback" experiment conducted at SCORE in August 2004. While the experimental results show that accurate horizontal location estimates can be easily obtained through a minimization of the misfit between the observed and predicted differences in the signal arrival times at a cluster of hydrophones, a high quality depth estimate is more difficult to accomplish. In order to choose a satisfactory estimator for the source depth, simulated data were used to systematically quantify the sensitivity of the source depth estimates, produced by a set of commonly used frequency and time-domain processing methods, to additive noise, sound speed profile (ssp) mismatch and hydrophone position errors. While all estimators proved tolerant to additive noise, a time domain "magnitude matching" estimator proved the most robust of the four investigated. This estimator was tolerant to a ssp mismatch up to 2 m/s (for a 100 m vertical extent feature located at 250 m depth) when combined with a hydrophone position error of 1 and 2 meters for two of the four hydrophones. The performance of this scheme was further demonstrated with experimental data. For source waveform estimation, the performance of a frequency-uncorrelated, least-squares technique was investigated. Computer simulation results show that the technique

2 This chapter is formatted for submission to the Journal of the Acoustical Society of America

requires a SNR > 5 dB and a sound-speed mismatch of < .1 m/s to work accurately. The insufficient SNR of the experimental data (~ -6 dB) prevented testing the technique with the actual data.

B. INTRODUCTION

The Navy requires a robust acoustic detection, localization and classification system to prevent inadvertent exposure of anthropogenic noise to marine mammals, including Odontocetes or "toothed" whales. Although visual surveys can be used for avoidance, this method is not continuously employed during military operations and is unfeasible at night or when visibility is restricted by fog or bad weather. Acoustic detection methods appear very promising, but for Odontocetes, specific challenges include high transmission losses (surface and bottom roughness scattering and chemical relaxation), significant variability inherent with Odontocete calls, and identification of specific species in the cacophony of high density, multiple animal vocalizations. An accurate and unambiguous three-dimensional localization algorithm would provide an excellent mitigation tool, most notably, at Navy acoustic ranges.

Matched field processing (MFP), matched signal processing (MSP) and time-difference-of-arrival localization of marine mammals has been conducted in several studies. Abawi *et al*. (2004) utilized MFP of acoustic data collected on an eight element vertical array (deployed from the Floating Instrument Platform (FLIP)) to localize and track singing Baleen whales during a seven day experiment at SCORE. Stafford *et al.* (1998) utilized MSP for long range and acoustic detection and localization of blue whale calls in the northeast Pacific Ocean. Specifically, a time domain matched filter was applied to recordings from three U.S. Navy SOund SUrveillance System (SOSUS) arrays to localize individual animals.

Time difference-of-arrival studies done by Clark *et al*. (1986/2000), Janik *et al*. (2000), and Mitchell *et al*. (1995) utilized time delay characteristics of multiple phone reception for baleen whale localization. Odontocete whistles have been successfully localized and tracked using a three-element hydrophone towed array (Thode, 2000), a sonobuoy array (Howarth, 2003), and through frequency domain beamforming using a

narrow aperture audio/video array (Ball and Buck 2003). Additional localization studies include Chiu and Miller (2004), Mellinger *et al*. (2000), Moore (1999), Thode *et al.* (2000), Tiemann (2001/2002/2003/2004), and Wiggins *et al.* (2004). Tiemann and Porter (2003) provided a concise comparison of time difference-of-arrival localization techniques as applied to marine mammal calls and found that model-based methods were favored when refractive effects were significant.

Previous work in source signal waveform reconstruction, specifically of blue whale calls, is outlined in research conducted by Thode *et al.* (2000) and Moore (1999). Thode utilized MFP and deconvolution techniques outlined in Finette *et al.* (1993) and Mignerey and Finette (1992) to localize and remove propagation effects from vocalizations received on a 48 element tilted vertical array. Source time signatures and source levels were then estimated. Moore conducted recordings on an eight hydrophone towed array and achieved retrieval of the source signature via least-squares fitting of modeled waveforms to received data.

C. OBJECTIVES / APPROACH

The objective of this study is to investigate the feasibility of using the near-bottom hydrophones of the U.S. Navy Southern California Offshore Range (SCORE) for three-dimensional localization of frequency-sweeping Odontocete vocalizations in the 10-20 kHz band and for reconstructing the source signal waveforms. Designed originally to track torpedoes and submarines during military exercises, the SCORE hydrophone array has exceptional potential for localizing those whistles that sweep within or through the designed bandwidth (~ 8-40 kHz) of the SCORE array.

The horizontal localization technique of this study is similar to a model-based approach used by Tiemann *et al* (2002), who achieved horizontal localization of vocalizing Humpback whales through a minimization of the misfit between the observed and predicted differences in the signal arrival times at an U.S. Navy Underwater Acoustic Range in Hawaii. The depth estimation and source signal reconstruction portion draws upon previous work done by Moore (1999) and Chiu *et. al* (2003). Moore localized a vocalizing blue whale using matched signal processing (MSP) as well as retrieval of the

source signature via least-squares fitting of modeled waveforms to received data. The Moore and Chiu studies focused on vocalizations at approximately 50 – 90 Hz and utilized a towed array. This study will focus on a much higher frequency regime (~10-20 kHz) and will utilize data collected from a carpeted array.

The approach entailed carrying out a playback experiment at the SCORE Range in August of 2004. It was followed by a computer simulated evaluation of commonly used frequency and time-domain processing methods for depth estimation. In order to choose a satisfactory estimator for the source depth, simulated data were used to systematically quantify the sensitivity of the source depth estimates to additive noise, environmental mismatch (sound speed error) and hydrophone positional error.

Briefly, the playback experiment transmitted a train of representative Odontocete (10-20-kHz) whistles using a J-9 sound source deployed from a research vessel to a depth of approximately 15 m. The transmissions were recorded at each hydrophone of a hexagonal sub-array consisting of seven near-bottom hydrophones. The playback experiment, including the geometry and the signaling and recording schemes, is detailed in Sec. D. Section D also outlines the synthesis of synthetic data using a four ray-path model, clarifies the formulation for the complex envelope of both data and predicted waveforms, and derives the narrowband approximation used for depth estimation. Section E outlines the derivation and experimental validation of a time-difference-of-arrival, model-based, horizontal localization scheme. Section F details the formulation and computer simulated sensitivity study of four time and frequency-domain depth estimators. The performance of the most robust scheme was further demonstrated with experimental data. For source waveform estimation, outlined in Sec. G., the formulation and computer simulated performance of a frequency-uncorrelated, least-squares estimator was investigated. Major conclusions of this study are given in Sec. H.

D. OBSERVED AND SYNTHETIC DATA

1. Data Collection - August 2004 Playback Experiment

a. Representative Odontocete Vocalization

The Research Vessel Point Sur, based out of Moss Landing, California, provided the research platform for this experiment. The goal of this experiment was to acoustically project a cycle of representative Odontocete whistles, as shown in Figure 1, for digital recording by the Range's bottom mounted hydrophones. The experiment was conducted from 11 to 13 August 2004 at the SCORE Underwater Acoustic Range. Hager (2008) describes the transmission sequence and data collection.

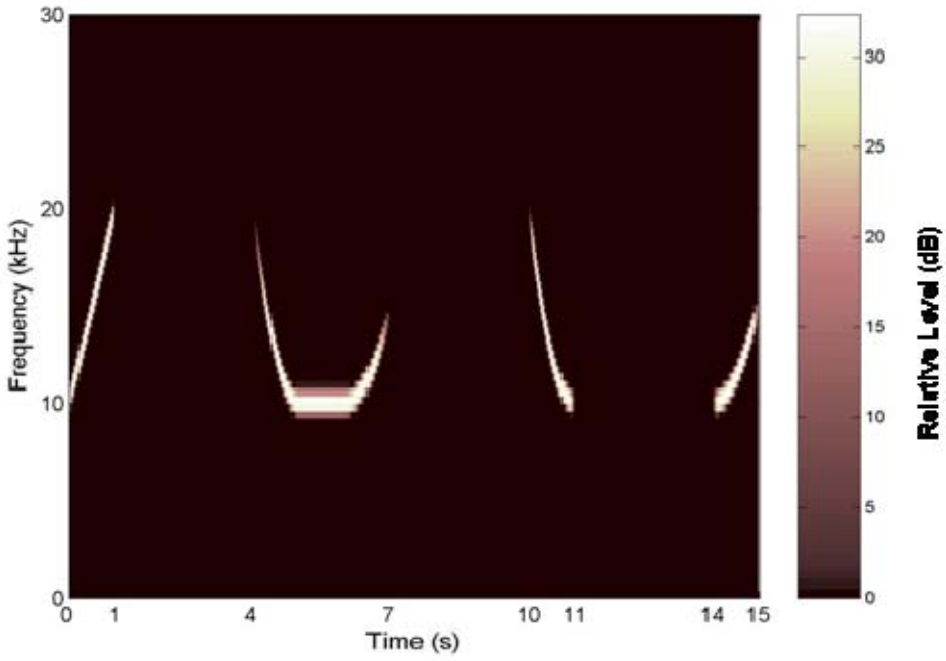

Figure 11. The spectrogram of the signal transmitted by the J9 sound source. The sequence consists of a 1 s, linear frequency-modulated (FM) "upsweep" and a succession of contoured, FM whistles. The linear upsweep was utilized in this study.

b. SCORE Underwater Acoustic Range Description

The SCORE Range is located on the western side of San Clemente Island. The water depths covered by the array vary from 1700 m in the northwest to 700 m in the southeast. The portion of the array utilized for this experiment includes hydrophones numbered 55, 61, 69, 70, 71, 77, and 78. They form a hexagon array with Hydrophone 70 in the middle location.

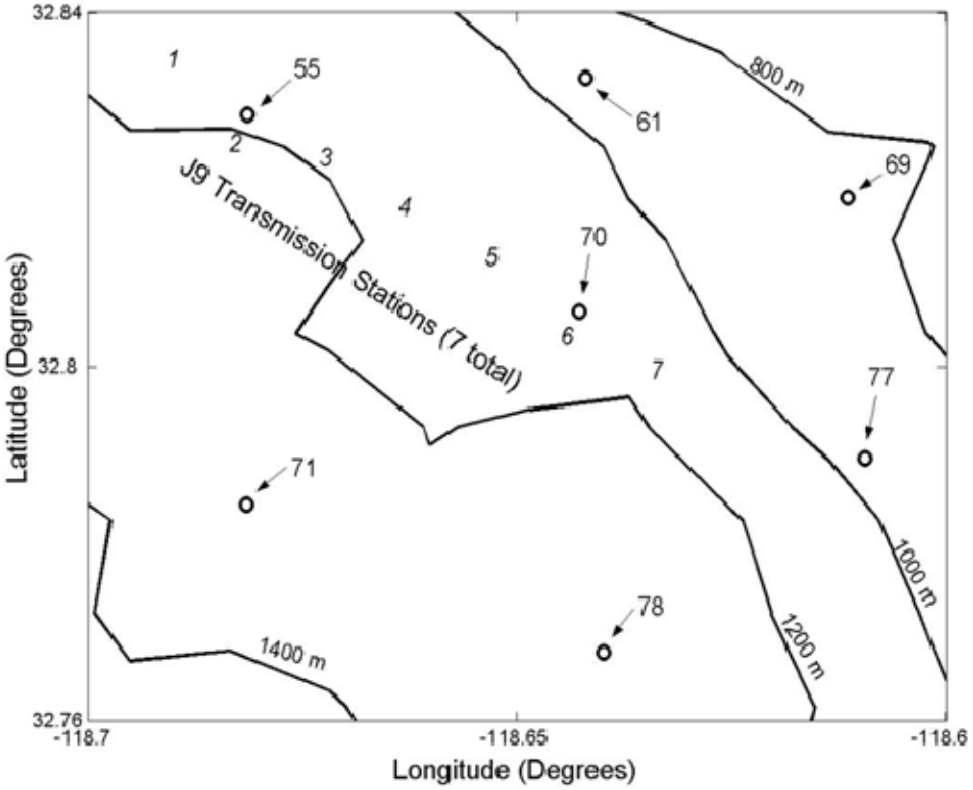

Figure 12. Geometry of the playback experiment showing locations of the seven transmission stations and nearby hydrophones. The isobaths are shown with a contour interval of 200 m.

The hydrophones in this subset array occupy depths varying from 1000 m to 1300 m. Based upon NOAA nautical charts, the bottom is composed of grey sand. According to table 1B of Hamilton (1980) (utilizing "very fine sand" and 50% porosity), the density of this sediment is 1.856 g/cm^3, with a sound speed of 1.702 km/s and attenuation of .68 dB/m/kHz.

2. Synthesis of Synthetic Data

a. Environmental Factors

Sippican expendable bathythermographs (XBTs) were deployed at each station during the experiment. XBT data collected from Station 6 and the synthetic or modeled sound speed profile is displayed in Figure 3. A strong downward refracting profile is evident. Historical data was utilized for the water column from the bottom of the XBT (~750 m).

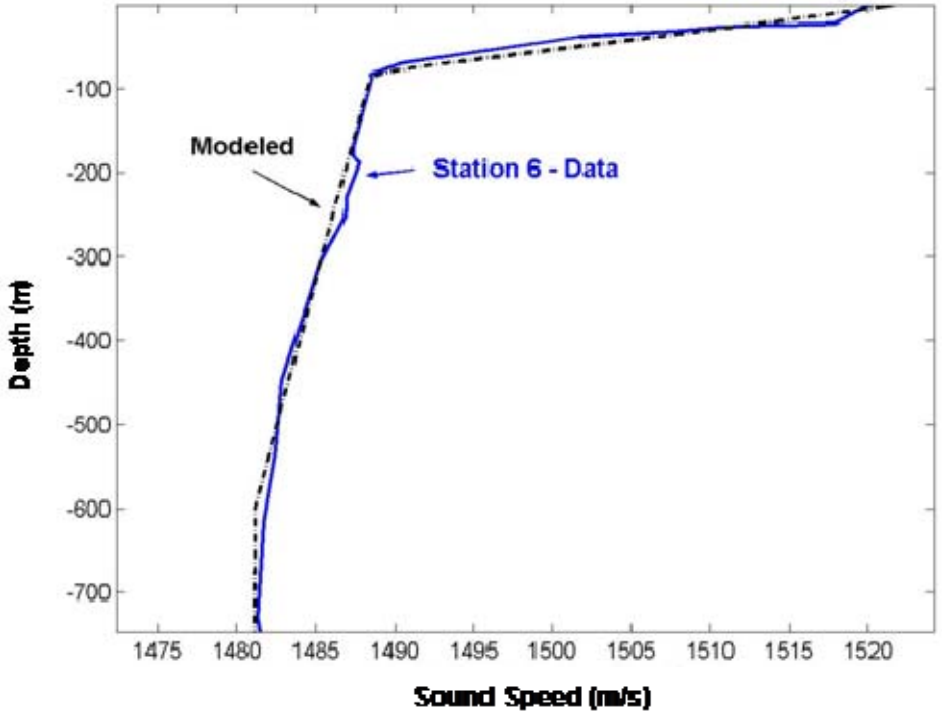

Figure 13. The sound speed profile used in the model (dashed) compared to data from the Station 6 Sippican expendable bathythermograph (XBT).

b. Use of the Complex Envelope and Notation

All subsequent formations of the various depth estimation schemes (Section F) being assessed presume that the input is either the complex envelope of the observed waveform or the frequency spectra of the complex envelope. Schemes attempting to match either the observed complex envelopes or their complex spectra with model predictions are commonly referred to as coherent methods, whereas those

attempting to match only the magnitudes of either the waveforms or spectra are referred to as incoherent methods. Through out the reminder of this paper, the superscript "*o*" is used to denote observed quantities, superscript *"m"* model predictions, subscript *"p"* hydrophone number, and the accent "~" complex envelopes or spectra of complex envelopes.

Using the aforementioned notation, the relation between the measured and modeled time series $r_p^o(t)$ and $r_p^m(t)$ and their complex envelopes $\tilde{r}_p^o(t)$ and $\tilde{r}_p^m(t)$ can be expressed as

$$r_p^o(t) = real\left[\tilde{r}_p^o(t)e^{i2\pi f_c t}\right] \text{ and } \quad r_p^m(t) = real\left[\tilde{r}_p^m(t)e^{i2\pi f_c t}\right] \qquad (1,2)$$

where f_c is the center frequency of the bandwidth of the signal. The complex envelope is a baseband signal, i.e., centered at zero Hz. All of the envelopes of the predicted waveforms are normalized by their root-mean-squared (RMS) value in the depth estimation portion of this study.

c. Use of the Narrowband Approximation

The Hamiltonian Acoustic Ray-Tracing Program for the Ocean (HARPO) was used to trace theoretical ray paths from the bottom mounted hydrophones. By numerical integration of the Hamilton's Equations, this program traces the paths of acoustic rays as they travel through an analytic model ocean. The original version of this program (Jones *et al.,* 1986) was upgraded in 1994 (Chiu *et al.,* 1994) to allow for the input of gridded bathymetry and sound speed data.

To simulate the acoustic arrival structure and invoking acoustic reciprocity, a vertical fan of rays was launched from each hydrophone along an azimuth to a distance of approximately 7 km. Identification of four specific eigenrays at incremental depth and range increments then allows for construction of arrival structure as a function of range and depth. The four ray paths utilized in the study were the direct path, a single surface reflection, a single bottom reflection, and the ray that experiences one surface and bottom reflection.

A MATLAB program developed by Chiu *et al.*, in 1994 was used to perform eigenray searches and compute signal amplitudes. This program calculates wave front travel times t_n and negative phase shifts ϕ_n along the ray paths and generates multi-path arrival structure. It requires RMS wave height, sediment density and sediment sound speed as inputs and conducts a coherent sum of the multi-path contributions to produce the predicted "receive" signal.

The "real" predicted received signal $r_p^m(t)$ is the inverse transform of the product between the source signal spectrum $S(f')$ and the modeled source to hydrophone transfer function $H_p^m(f')$,

$$r_p^m(t) = \int_{-\infty}^{\infty} S(f')H_p^m(f')e^{i2\pi f' t}df' , \qquad (3)$$

where

$$H_p^m(f') = \sum_{n=1}^{4} a_n(f')e^{-i(2\pi f' t_n \pm \varphi_n)} . \qquad (4)$$

In (4), N=4 is the number of eigenrays and f' is the actual frequency. Additionally, the amplitude a_n, in general, is a function of frequency accounting for ray tube spreading, surface scattering loss, bottom reflection loss and volume attenuation due to chemical relaxation. The $\pm$ values in the exponential correspond to frequencies greater than and less than zero respectively.

Following (1), (2), (3) and (4), the complex envelope of the modeled received signal $\tilde{r}_p^m(t)$ is then

$$\tilde{r}_p^m(t) = \sum_{n=1}^{4} \int_{-\infty}^{\infty} S(f')a_n(f')e^{-i(2\pi f' t_n + \varphi_n)}e^{i2\pi f' t}e^{-i2\pi f_c t}df' \qquad (5)$$

where the spectrum is moved to baseband. Denoting f as the baseband frequency with

$$f = f' - f_c , \qquad (6)$$

$\tilde{r}_p^m(t)$ can be recast as

$$\tilde{r}_p^m(t) = \sum_{n=1}^{4} \int_{-\infty}^{\infty} \tilde{S}(f) a_n(f_c + f) e^{-i(2\pi f_c t_n + \varphi_n)} e^{i2\pi ft} df \ , \qquad (7)$$

where

$$\tilde{S}(f) = S(f_c + f) \ . \qquad (8)$$

Applying a narrowband approximation, where a_n is assumed constant around f_c, (7) becomes

$$\tilde{r}_p^m(t) \cong \sum_{n=1}^{4} \left[\int \tilde{S}(f) e^{-2\pi ft_n} e^{i2\pi ft} df \cdot a_n e^{-i(2\pi f_c t_n + \varphi_n)} \right]. \qquad (9)$$

Invoking the time-delay property in Fourier transform and writing out the dependency on source location (x_s, y_s, z_s), the narrowband approximation (8) can be recast as

$$\tilde{r}_p^m(t; x_s, y_s, z_s) = \sum_{n=1}^{4} \tilde{s}(t - t_n) a_n e^{-i(2\pi f_c t_n + \varphi_n)} \ . \qquad (10)$$

This approximation is applicable to the source-depth estimation portion of this study because only a portion (.1 s) of the one second linear sweep was utilized for both predicted and observed waveforms.

E. HORIZONTAL LOCALIZATION

1. Previous Work / Background

Horizontal localization of marine mammal vocalizations with widely separated hydrophones can easily be accomplished utilizing time difference-of-arrival (time-lag) techniques. Tiemann *et al*. (2003) developed / utilized an algorithm of this type to track Humpback whales using a deep water array near Hawaii. A range-dependent acoustic model was used to predict time-lags expected at each sensor within the array, while observed time-lags were measured through a phase-only correlation process. An ambiguity surface (in the horizontal plane) was then used to compare observed and predicted time-lags and display the most probable whale location.

A similar technique is utilized in this study. A cross correlation of the observed signal to the synchronous recordings of the three remaining hydrophones resulted in *observed* time-lags. These time-lags, when compared to a search grid of *predicted* time-lags can reveal a horizontal position.

2. Formulation and Results

Given the known hydrophone positions (x_p, y_p) and the position of the nearest hydrophone (x_{ref}, y_{ref}) to possible source locations on the search grid (x_s, y_s), the predicted time-lags or "lags," $\tau_p(x_s, y_s)$, are calculated as

$$\tau_p^m(x_s, y_s) = \sqrt{\left|x_s - x_p\right|^2 + \left|y_s - y_p\right|^2}\,/\,c - \sqrt{\left|x_s - x_{ref}\right|^2 + \left|y_s - y_{ref}\right|^2}\,/\,c\,. \qquad (11)$$

A least-squares solution can minimize the error between the three observed (data) lags τ_p^o and the predicted lags $\tau_p^m(x_s, y_s)$. The least squares misfit function is

$$a(x_s, y_s) = \frac{1}{3}\sum_{p=1}^{3}\left[\tau_p^o - \tau_p^m(x_s, y_s)\right]^2. \qquad (12)$$

The best positional estimate is where $a(x_s, y_s)$ is a minimum.

This misfit function can also be referred to as an ambiguity surface. As an example, Figure 4 displays the ambiguity surface for one of the playback signals transmitted at Station 5. This localization compares favorably with the truth. This method consistently worked well in localizing other playback transmissions.

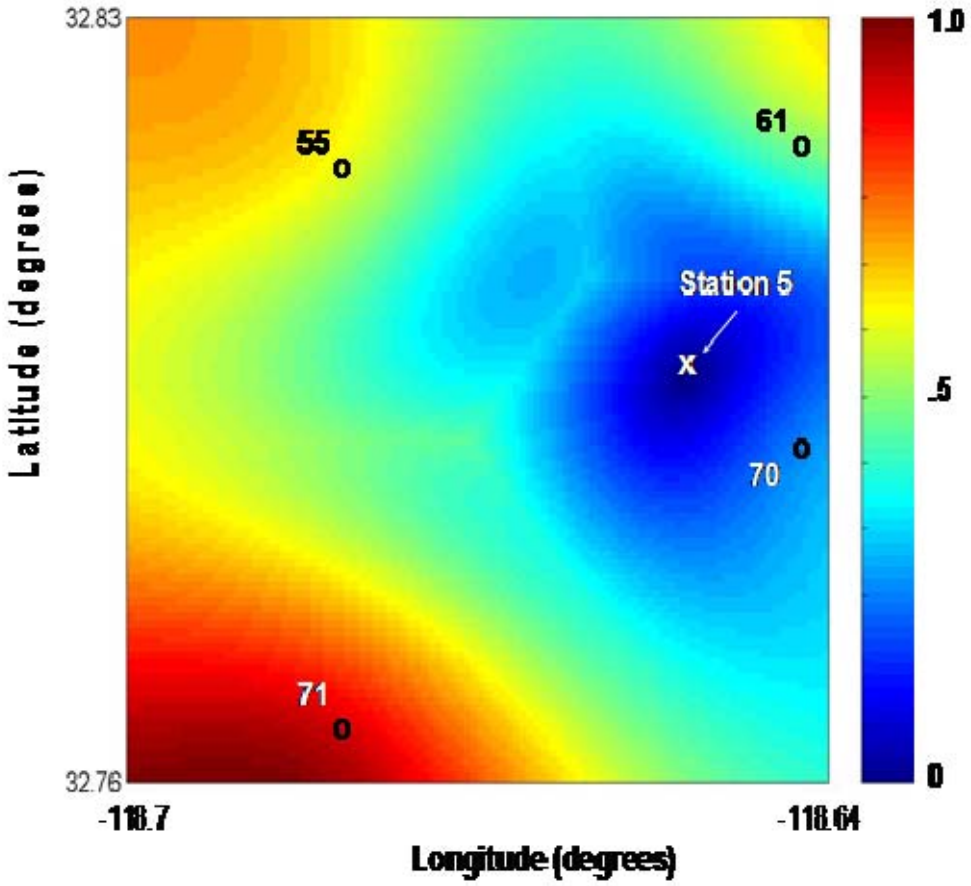

Figure 14. Ambiguity surface for a playback signal transmitted at Station 5. The color bar shows the error between observed and predicted lags. The best estimate, shown as an 'X' on the grid, was accurately localized in this example. The search grid encompassed an area of approximately 49 km^2.

F. DEPTH ESTIMATION

1. Estimator Formulation

a. Frequency Uncorrelated Matched Field Processing (FUMFP)

The Bartlett (linear) processor is utilized here to establish the equations for a coherent and an incoherent scheme in the frequency domain. The Bartlett processor correlates the observed spectra $\tilde{R}_p^o(f)$, where f is the baseband frequency, with a set of

predicted spectra, $\tilde{R}_p^m(f;z_s)$, that are often called "replicas" in MFP literature. For depth estimation, the replicas are calculated using a propagation model for a set of possible source depths, z_s, on a vertical search grid. The property of reciprocity of the sound field can be used to save computational time in the generation of the replicas.

For coherent processing and adopting Tolstoy (1993) notation, the processor output can be expressed as

$$P_{linear}(z_s;f) = \underline{w}^{+}\underset{\sim}{C}\underline{w}, \qquad (13)$$

where the superscript "+" denotes transpose and complex conjugate, and

$$\underline{w} = \begin{bmatrix} \tilde{R}_{69}^m(f;z_s) \\ \tilde{R}_{70}^m(f;z_s) \\ \tilde{R}_{77}^m(f;z_s) \\ \tilde{R}_{78}^m(f;z_s) \end{bmatrix} \qquad (14)$$

is a vector containing the predicted spectral values at the four hydrophones for a frequency of *f* and a trial source depth. In (13), the cross-spectral data matrix, $\underset{\sim}{C}$, of size 4 by 4, can be calculated as

$$\underset{\sim}{C} = \underline{\underline{F}}\underline{\underline{F}}^{+}, \qquad (15)$$

where

$$\underline{\underline{F}} = \begin{bmatrix} \tilde{R}_{69}^o(f) \\ \tilde{R}_{70}^o(f) \\ \tilde{R}_{77}^o(f) \\ \tilde{R}_{78}^o(f) \end{bmatrix} \qquad (16)$$

is a data vector containing the observed spectral values at the same frequency.

By replacing the complex values $\tilde{R}_p^m(f;z_s)$ and $\tilde{R}_p^o(f)$ in (14) and (16) with their respective magnitudes, i.e., $\left|\tilde{R}_p^m(f;z_s)\right|$ and $\left|\tilde{R}_p^o(f)\right|$, the processor expressed in (13) becomes an incoherent estimator. Whether processing coherently or incoherently, $P_{linear}(z_s;f)$ at each frequency "bin" represents a similarity measure as a function of trial source depth. A larger value in P_{linear} corresponds to a better match between model prediction and observation and vice versus. The best source depth estimate is where the

frequency-averaged (over all bins) P_{linear} attains maximum. Following convention, the averaged P_{linear} is referred to as the ambiguity curve in this study because multiple maxima of approximately equal amplitude, if they exist, would give an ambiguous source depth estimate.

b. Time Domain Matched Signal Processing (TDMSP)

TDMSP processing was accomplished utilizing two schemes – "waveform correlation" (coherent) and "magnitude matching" (incoherent). Waveform correlation is accomplished as

$$c_{\underline{\tilde{r}}^o \underline{\tilde{r}}^m}(\tau; z_s) = \frac{1}{N} \int \underline{\tilde{r}}^o(t; z_s)^+ \underline{\tilde{r}}^m(t+\tau; z_s) dt \,, \qquad (17)$$

utilizing the complex envelope vectors

$$\underline{\tilde{r}}^o(t; z_s) = \begin{bmatrix} r^o{}_{69}(t; z_s) \\ r^o{}_{70}(t; z_s) \\ r^o{}_{77}(t; z_s) \\ r^o{}_{78}(t; z_s) \end{bmatrix} \text{ and } \underline{\tilde{r}}^m(t; z_s) = \begin{bmatrix} r^m{}_{69}(t; z_s) \\ r^m{}_{70}(t; z_s) \\ r^m{}_{77}(t; z_s) \\ r^m{}_{78}(t; z_s) \end{bmatrix} \qquad (18,19)$$

with + representing the complex conjugate and transpose. The predicted waveforms $\underline{\tilde{r}}^m(t; z_s)$ in (19) were calculated from (10). Magnitude matching was accomplished as

$$c_{\left|\underline{\tilde{r}}^o\right\|\underline{\tilde{r}}^m\right|}(\tau; z_s) = \frac{1}{N} \int \left|\underline{\tilde{r}}^o(t; z_s)\right|^T \left|\underline{\tilde{r}}^m(t+\tau; z_s)\right| dt \qquad (20)$$

with *T* representing the transpose. The maximum value of correlation output (17,20) over τ and at each depth is displayed as an ambiguity curve in subsequent figures. The peak value of the ambiguity curve provides the best depth estimate. Each scheme assumed the source amplitude was approximately constant over a very small fraction (.1 s) of the entire signal duration (1 s). This is consistent with the narrowband approximation.

2. FUMFP Computer Simulated Sensitivity Study

a. Additive Noise

This section introduces the first of three sensitivity studies, specifically to quantify the simulated effects of adding stationary white noise on the performance of the FUMFP estimators. The remaining studies will focus on sound speed mismatch and the combined effects of hydrophone position error and sound speed error. The ultimate goal of this chapter is to provide threshold (maximum tolerable) values in order to achieve an unambiguous and accurate depth estimate for each of the three sensitivity studies.

Stationary white noise implies that it is frequency uncorrelated. Because of this, a "gain" is experienced by frequency averaging the processor output for display as an ambiguity curve. This gain can be as high as

$$\text{Gain}_{\text{freg avg}} = 10\, log_{10}(M), \qquad (21)$$

where M is the number of frequencies. Given the number of frequencies utilized in this processor, a 23 dB (M=200) increase in SNR can be experienced. Theoretically, this would imply that the required SNR would increase without bound as the number of frequencies increased. It is important to note, however, that real-world noise is not perfectly uncorrelated in frequency.

Figure 5 displays the "unlimited" SNR and additive noise ambiguity curves for a four hydrophone, FUMFP coherent estimator. The difference between the estimate and the controlled true location is a measure of accuracy. The difference between the magnitudes of peak processor output compared to adjoining side lobes is a measure of ambiguity.

In simulation, both estimators proved robust in response to additive noise. Frequency averaging significantly enhanced the SNR threshold of both estimators by reducing side lobes. This simulation indicates that the FUMFP processors will produce an unambiguous and accurate estimate as long as SNR is greater than -25 dB for the

coherent estimator and -20 dB for the incoherent estimator (not shown) when the processor output is frequency averaged.

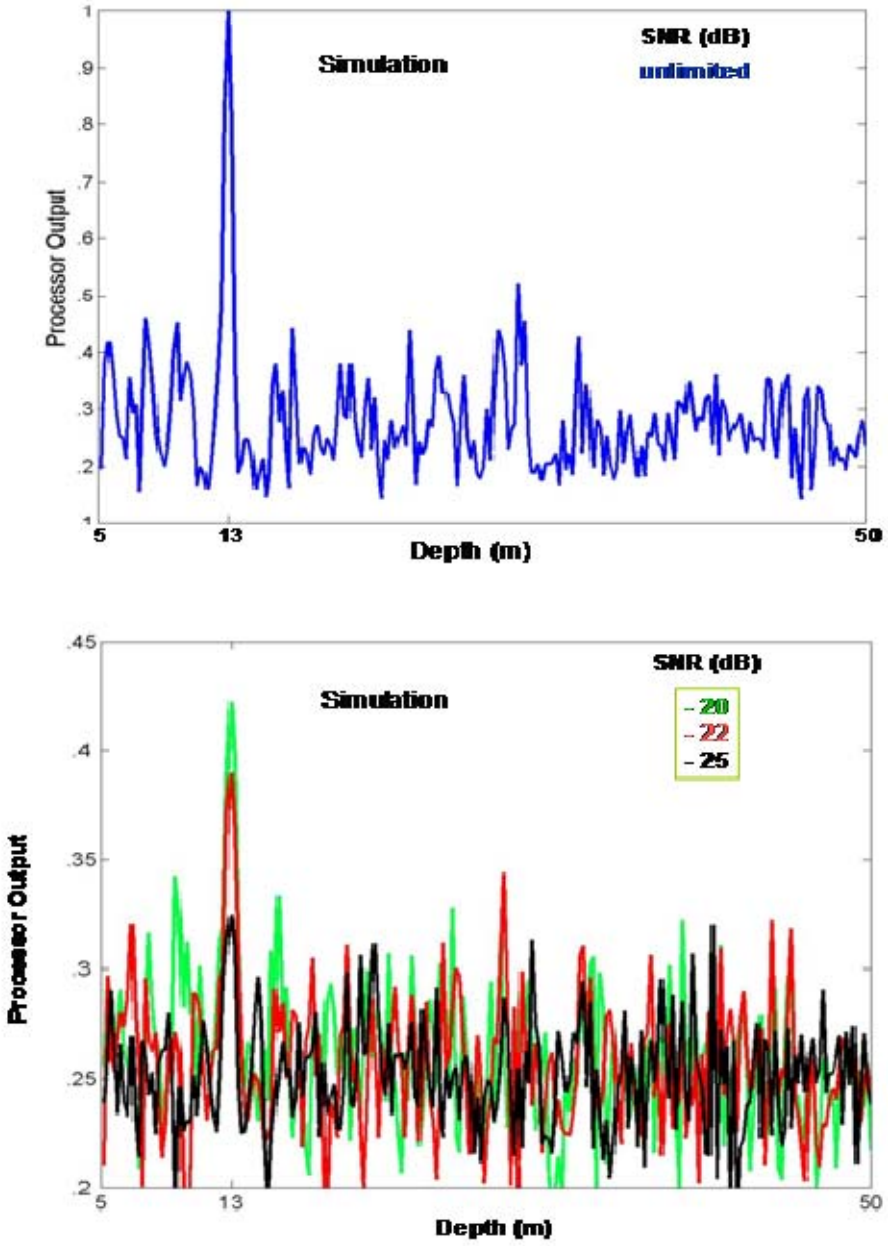

Figure 15. Four hydrophone FUMFP coherent estimator ambiguity curves in an unlimited SNR environment (top panel) and in response to additive noise (lower panel). The peak value represents the depth estimate. Frequency averaging gain is included in the lower panel.

b. Sound Speed and Hydrophone Position Error

Given a known horizontal position (x_s, y_s), the modeled received signal $\tilde{r}_p^m(t; z_s)$, can be calculated from (10). The center frequency, travel time product $f_c t_n$ in the phase, however, is sensitive to travel time error caused by mismatch between the modeled and actual sound speed profile (sound speed error). This sound speed error $\delta c(z)$, is

$$\delta c(z) = c^o(z) - c^m(z) \ . \qquad (22)$$

In order to simulate the travel time error resulting from this type of mismatch, a synthetic (vertical extent or Δh = 100 m) sound speed profile anomaly or "feature" (Figure 6) that produced sound speed errors of .1, .2 and 1 m/s was introduced into the model. The corresponding "j^{th}" eigenray time travel error δt_j, is then calculated as

$$\delta t_j = -\int \frac{\delta c(z)}{\left(c^m\right)^2} ds \, . \qquad (23)$$

Collectively, these travel time errors lead to error in the predicted received signal.

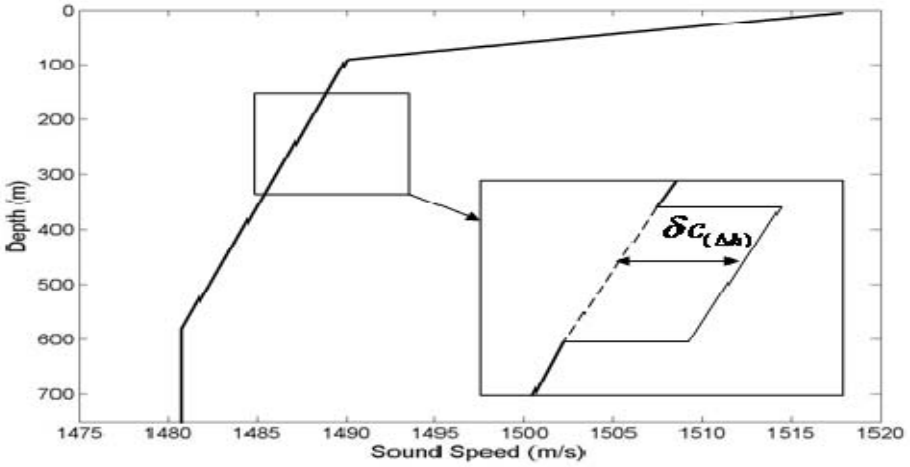

Figure 16. Synthetic sound speed profile "feature" located at 250 m depth (Δh refers to the vertical extent of the feature).

The simulated results are displayed in Figure 7. It is clearly evident that the coherent estimator can't tolerate sound speed errors caused by this feature greater than .1 m/s. The performance is even poorer for the incoherent estimator.

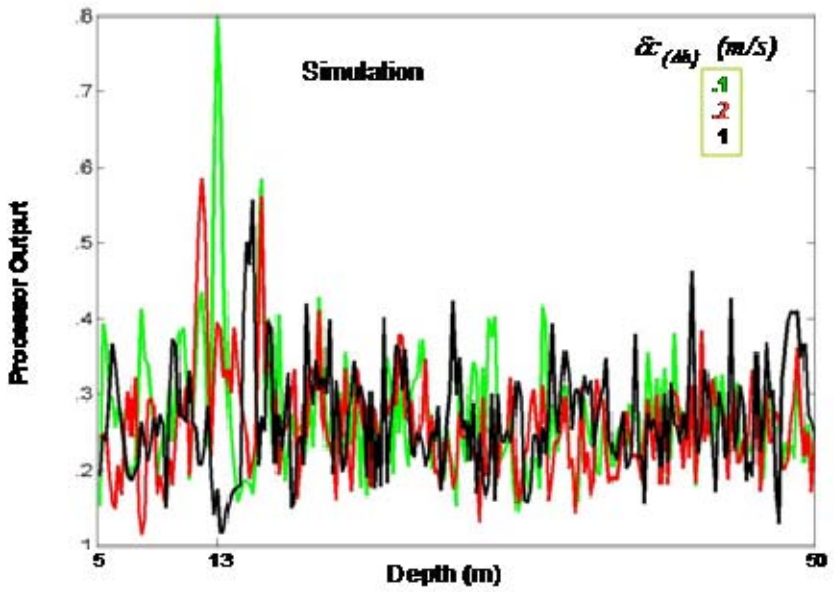

Figure 17. Four hydrophone, FUMFP coherent processor ambiguity curves are displayed for a 1 kHz portion of the upsweep. Sound speed error values of .1, .2 and 1 m/s experienced over a 100 m feature located at a depth of approximately 250 m were investigated. The true source depth used for simulation was 13 m.

FUMFP sensitivity to hydrophone positional error *and* additive sound speed error is displayed in Figure 8. The induced positional error was accomplished by holding two hydrophone depths constant and adjusting the depths of the remaining two hydrophones by 1 m and 2 m respectively. The computer simulation was then re-run with 0 and .1 m/s sound speed error. The accuracy of the estimate suffered with greater than a .1 m/s error. For example, even though the 1 m/s ambiguity curve provided an unambiguous estimate, it was approximately 3 meters in error.

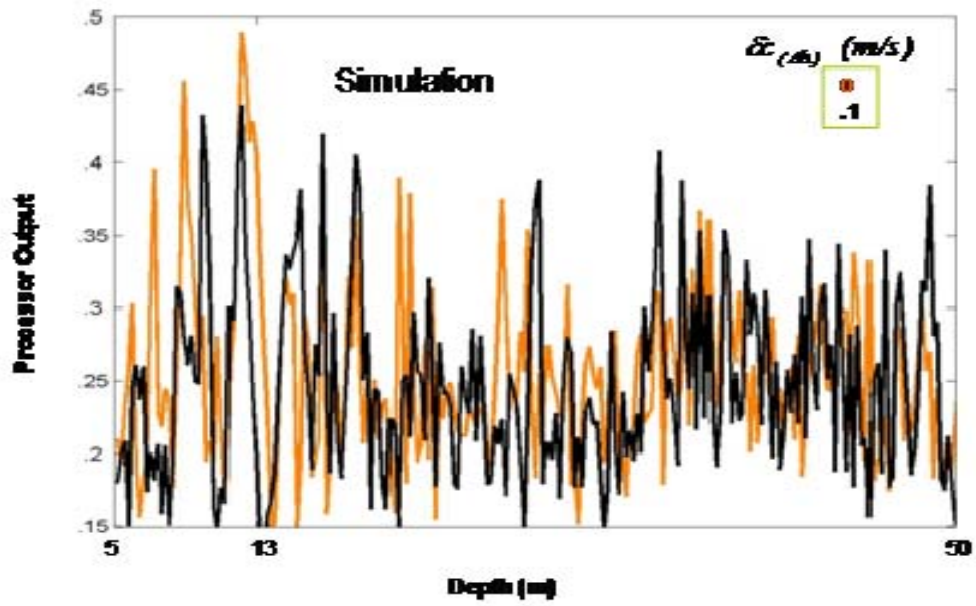

Figure 18. The combined effects of 1 m and 2 m hydrophone vertical positional error (for two of four total hydrophones) and sound speed error values of 0 and .1 m/s experienced over a 100 m feature located at a depth of approximately 250 m for a four hydrophone, FUMFP coherent estimator. The true source depth used for simulation was 13 m.

While the positional errors alone (given $\delta c_{(\Delta h)}$ = 0 m/s) significantly degraded depth estimation in the coherent estimator (Figure 8), an unambiguous depth estimate could not be made with the incoherent scheme. The combined effects of hydrophone position (1 m and 2 m vertical position error over 1400 m depth for two of four hydrophones) and sound speed error clearly affect the performance of these estimators. Based upon the limited tolerance of both processors, they are both inadequate for depth estimation.

3. TDMSP Computer Simulated Sensitivity Study

Although both four hydrophone, TDMSP schemes were found to be robust in response to additive noise (-22 dB for waveform correlation and -10 dB for magnitude matching), waveform correlation proved especially sensitive to sound speed error alone and accurate results were not obtained - even for the starting value of .1 m/s. The

magnitude matching estimator, however, provided an accurate and relatively unambiguous depth estimate for up to 3 m/s of sound speed error (Figure 9).

When the hydrophone positional errors induced in the previous section were combined with sound speed error, the estimator performed nearly as well and provided an accurate and unambiguous depth estimate up to 2 m/s of sound speed error (Figure 10). Although additional increments of sound speed error revealed an unambiguous depth estimate (specifically 5 m/s in Figure 9 and 4 m/s in Figure 10), they were inconsistent. Based upon the sensitivity study results from this and previous sections, the four hydrophone TDMSP magnitude matching estimator was found to be the most tolerant and accurate of the four analyzed.

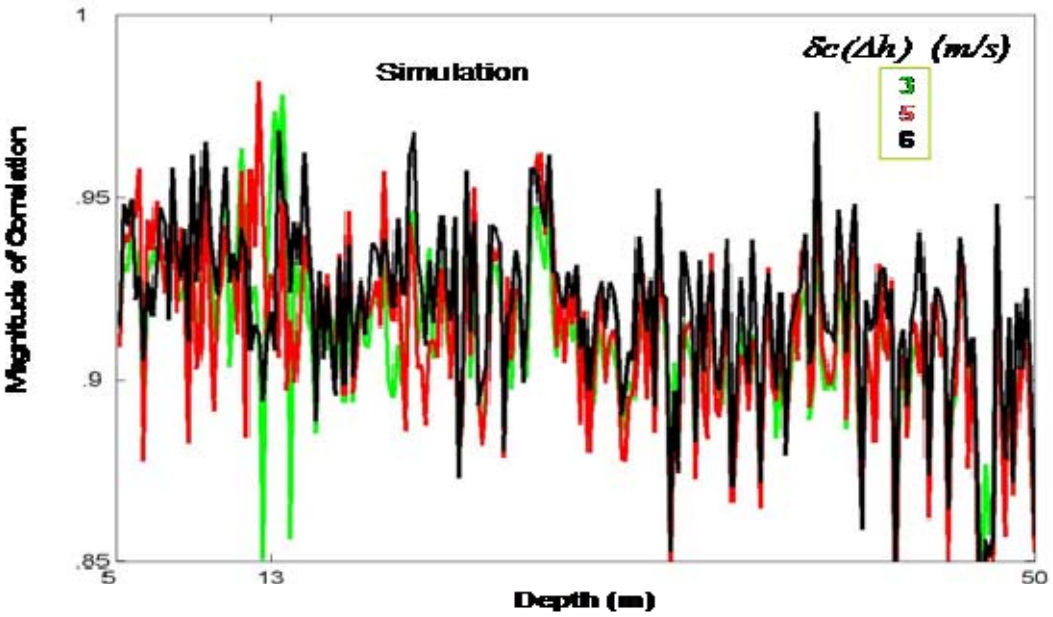

Figure 19. Four hydrophone (N=4) TDMSP magnitude matching estimator results in response to sound speed error values of 3, 5 and 6 m/s experienced over a 100 m feature located at a depth of approximately 250 m. The true source depth used for simulation was 13 m.

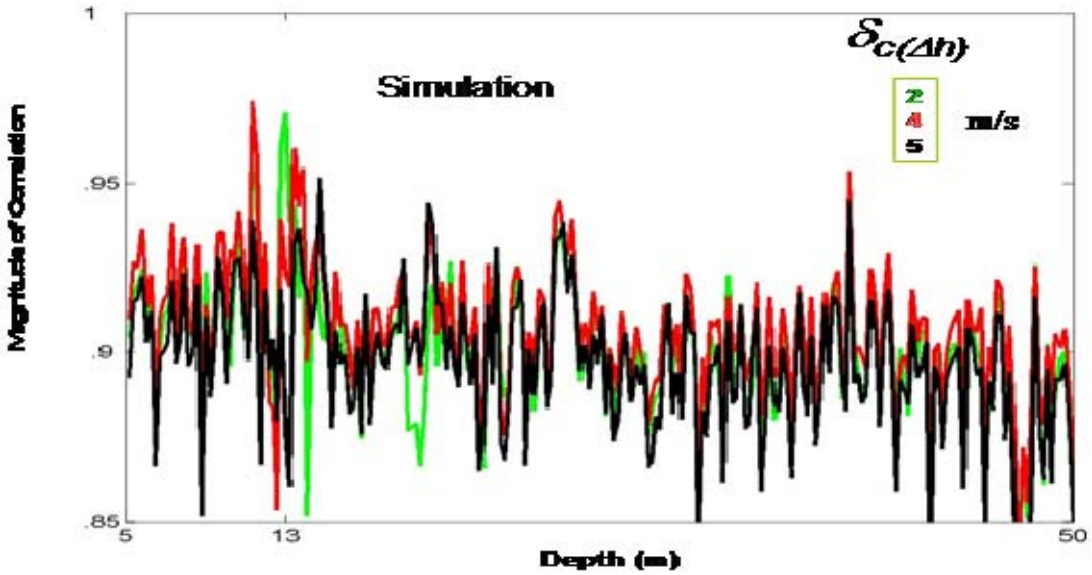

Figure 20. Four hydrophone (N=4) TDMSP magnitude matching estimator results in response to 1 m and 2 m hydrophone vertical positional errors (for two of four total hydrophones) and sound speed error values of 2, 4, & 5 m/s experienced over a 100 m feature located at a depth of approximately 250 m. The true source depth used for simulation was 13 m.

4. Experimental Results

When the magnitude matching estimator was applied to data, a peak at the known approximate depth resulted (Figure 11). An additional peak, however, is apparent at 38 m. The bimodal nature of these results indicates that at least one of the tolerances was exceeded.

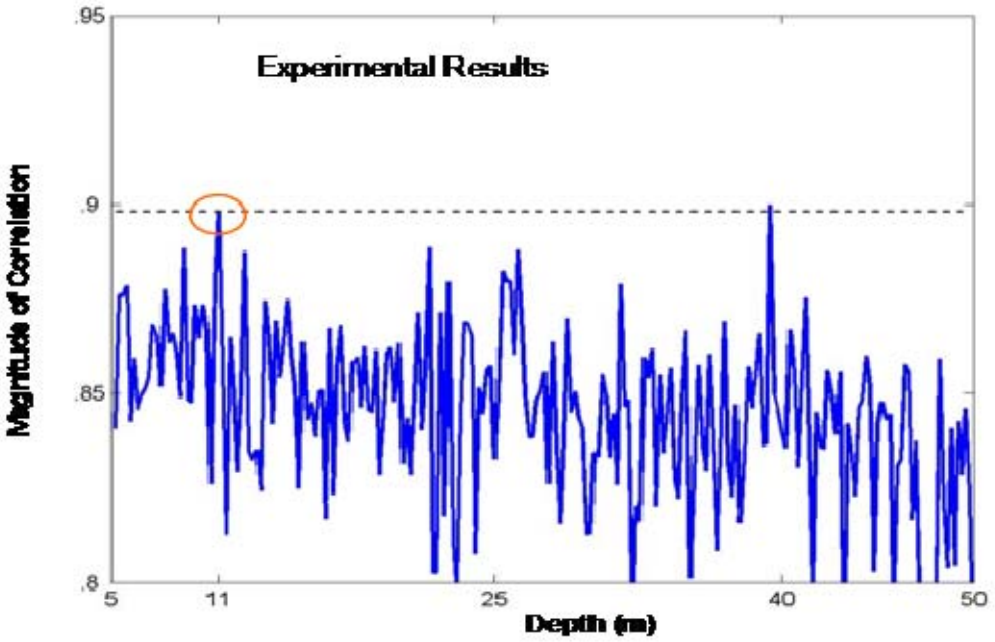

Figure 21. Four hydrophone (N=4) TDMSP magnitude matching estimator results. The red circle indicates the peak closest to known depth.

In an attempt to achieve an unambiguous result, *N* was reduced from four to one. In doing so, *individual* hydrophone ambiguity curves did provide unambiguous estimates, but the depths were inconsistent. Figure 12 displays single hydrophone (*N*=1) magnitude matching, ambiguity curves for Hydrophones 69, 77 and 78. The peak value for Hydrophone 69 is 11.8 m, 10.6 m for Hydrophone 78 and 20.8 m for Hydrophone 77.

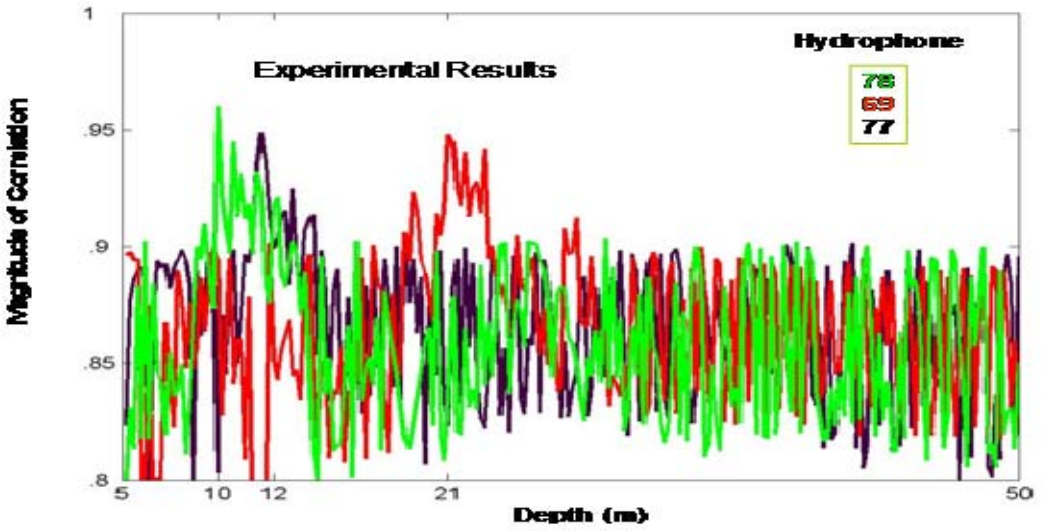

Figure 22. Single hydrophone (N=1) TDMSP magnitude matching estimator results for Hydrophones 69, 77 and 78. The inconsistent peaks, or depth estimates, reveal the potential hydrophone positional and/or sound speed error.

Further analysis as to the cause for the inconsistent depth estimates was accomplished by varying the two suspected parameters (hydrophone position and sound speed error) independently in computer simulation. The single hydrophone estimator proved robust to sound speed error (Figure 13), but was very sensitive to hydrophone position error (Figure 14). Introduction of a 6 m vertical position error resulted in nearly a 5 m difference from the zero position error result. This positional error, suspected in earlier computer simulation sections as potentially degrading performance, is suspected as the cause for the inconsistent peaks found in the experimental single hydrophone TDMSP magnitude matching results.

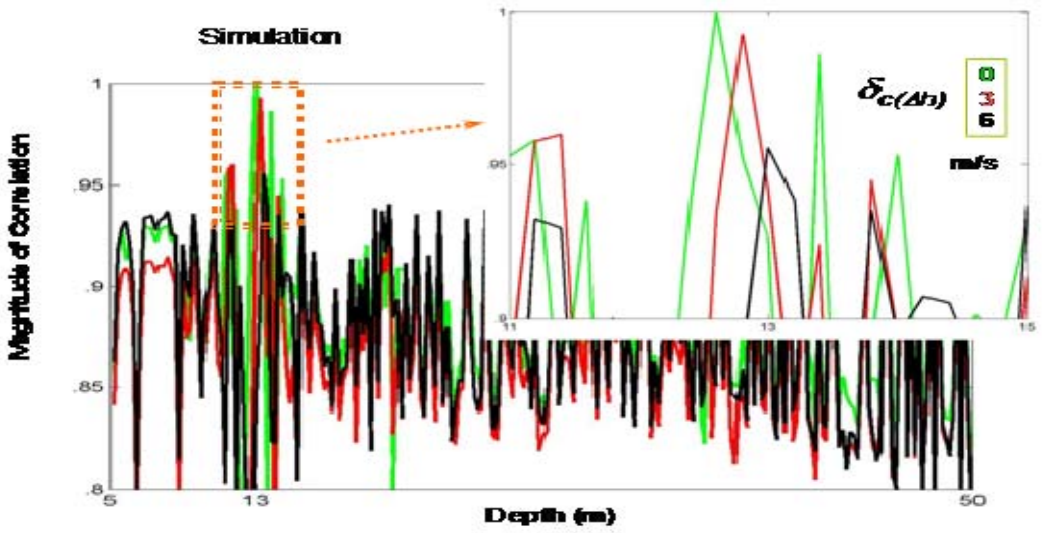

Figure 23. Hydrophone 69 TDMSP magnitude matching estimator results with sound speed error values of 0, 3 and 6 m/s experienced over a 100 m feature located at a depth of approximately 250 m. The true source depth used for simulation was 13 m.

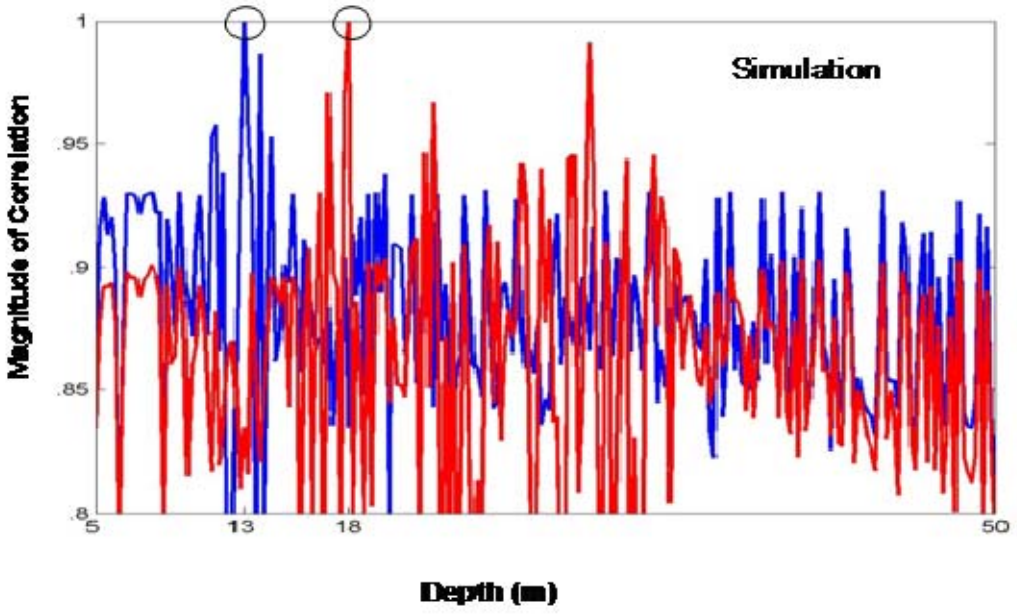

Figure 24. Hydrophone 69 TDMSP magnitude matching estimator results with zero and a 6 m position error. The true source depth used for simulation was 13 m.

G. SOURCE SIGNAL WAVEFORM RECONSTRUCTION

1. Least Squares Estimation Formulation

Given the three dimensional estimated position corresponding to longitude, latitude, and depth, the next sequential step in this study was to attempt a source signal waveform reconstruction. Although fixed bottom hydrophones do not often afford the opportunity for unaltered, near field digital recording, a modeled field of expected source to hydrophone transfer functions, combined with received data from multiple hydrophones, can be utilized for a least-squares estimate of the source signal waveform. Reconstruction of the source signal amplitude modulation, specifically the magnitude of the complex envelope, is the goal.

Following the technique outlined in Moore (1999) and Chiu *et al*. (1999), the frequency spectrum $\tilde{R}_p(f)$ of the signals received at the *"p^{th}"* hydrophone is related to the frequency spectrum of the source signal $\tilde{S}(f)$, weighted by the source-to-receiver transfer functions $\tilde{H}_p(f)$ combined with the additive effects of noise $\tilde{N}_p(f)$. This is stated mathematically as

$$\tilde{R}_p(f) = \tilde{S}_p(f)\tilde{H}_p(f) + \tilde{N}_p(f). \qquad (24)$$

The best estimate of the source signal's frequency spectrum $\hat{\tilde{S}}(f)$, assuming no known signal characteristics, is then calculated through least-squares estimation.

In this technique, the sum of squared errors or cost function, *C*, is calculated as

$$C = \left[\underline{\tilde{R}}_p^o(f) - \underline{\tilde{H}}_p^m(f)\tilde{S}(f)\right]^+ \left[\underline{\tilde{R}}_p^o(f) - \underline{\tilde{H}}_p^m(f)\tilde{S}(f)\right], \qquad (25)$$

where $^+$ represents the conjugate transpose. The cost function is minimized to obtain the best estimate of the source signal spectrum in

$$\hat{\tilde{S}}(f) = \left[\underline{\tilde{H}}^m(f)^+ \underline{\tilde{H}}^m(f)\right]^{-1} \underline{\tilde{H}}^m(f)^+ \underline{\tilde{R}}^o(f) \qquad (26)$$

The best estimate of the source signal $\hat{\tilde{s}}(t)$ is then calculated via the inverse transform of $\hat{\tilde{S}}(f)$ as

$$\hat{\tilde{s}}(t) = \int \hat{\tilde{S}}(f) e^{-i2\pi ft} df \ . \qquad (27)$$

It is important to note that this deverberation method is frequency-uncorrelated, specifically, the least squares estimate is conducted bin-by-bin, with no relationship to adjoining bins.

2. Source Signal Reconstruction Sensitivity Study

Figure 15 displays the least-squares estimator's response to additive noise while Figure 16 shows the estimator's response to sound speed error. The ramp-up and ramp-down slopes and constant amplitude modulation are evident in all reconstructed waveforms for the noise study as long as the SNR remains above 5 dB. The magnitude of the complex envelope is clearly evident in the 10 dB panel.

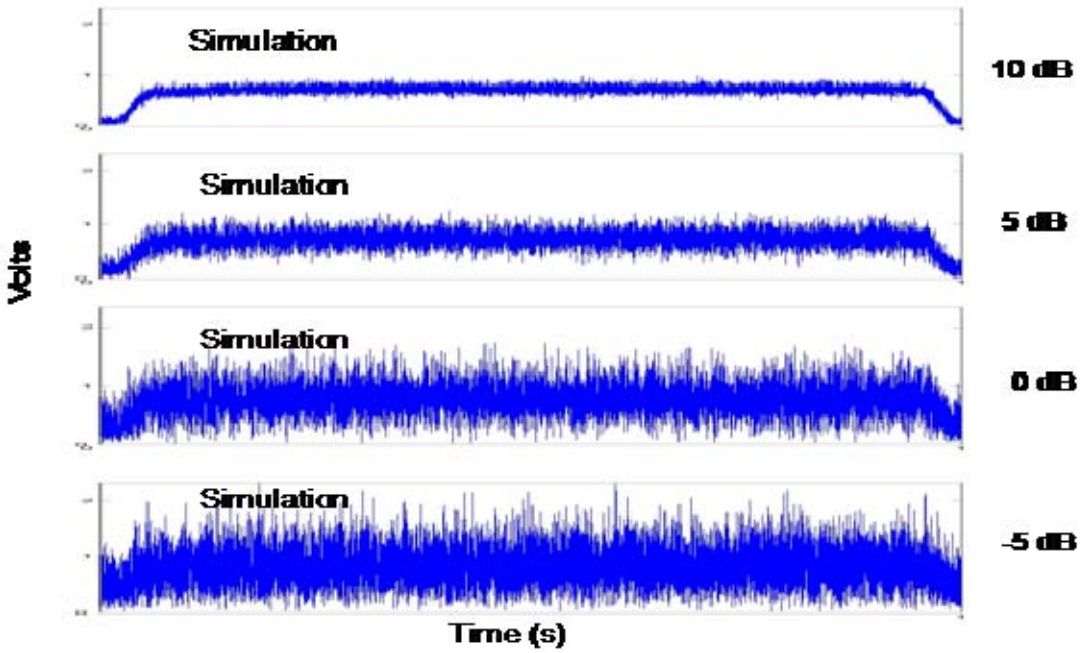

Figure 25. Four hydrophone, frequency-uncorrelated least-squares, source signal waveform estimator results in response to additive noise. SNR decreases from top to bottom. The source signal waveform is 1 s in duration.

Figure 16 displays the computer simulation of added sound speed error effects on the least squares estimator. The magnitude of the complex envelope with zero error is displayed for comparison in the top panel. The ramp-up and ramp-down slopes remain

evident in response to elevated sound speed error values, but there is a significant deviation from the constant amplitude between the slopes. This estimator appears sensitive to sound speed errors greater than .1 m/s.

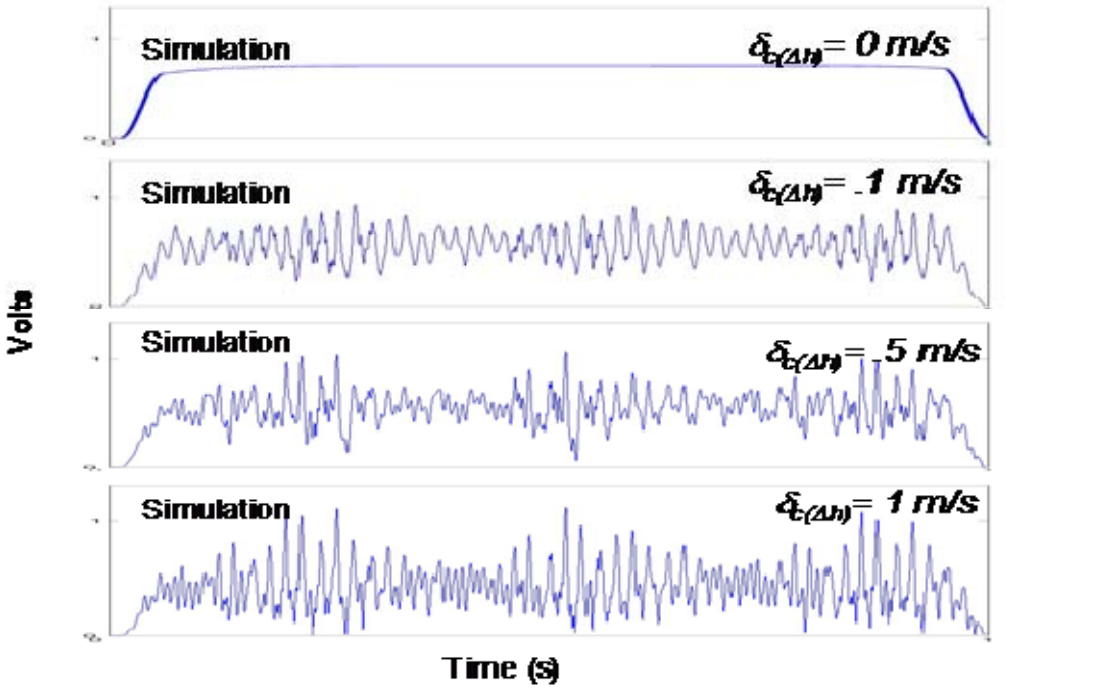

Figure 26. Four hydrophone, frequency-uncorrelated least-squares, source signal waveform estimator results in response to sound speed error. Error values of .1, .5 and 1 m/s experienced over a 100 m feature located at a depth of approximately 250 m are presented. The source signal waveform is 1 s in duration.

There is a potential to achieve a better tolerance or lower SNR with this estimator by incorporating "*a priori*" parameters. Frequency bandwidth, phase modulation and signal duration can be revealed with spectrograms. *A priori* constraints could be included in future work.

Experimental results obtained with a three hydrophone least-squares estimator were inconclusive. Hydrophone 70 observed data was not utilized in the estimator due to an AGC change. This limitation, detailed in Hager (2008) poses a significant challenge not only to waveform reconstruction, but SL calculations as well.

Unfortunately, neither the ramp-up / ramp-down slopes nor the constant amplitude were reconstructed. A number of reasons are suspected. The most probable reasons are the combined affects of additive noise, sound speed error and hydrophone positional inaccuracies.

H. SIGNIFICANT RESULTS / CONCLUSIONS

1. Depth Estimation

a. Simulated Results - FUMFP

While both FUMFP estimators proved equally robust in response to additive noise, the coherent estimator produced unambiguous and accurate results, with significant side-lobe suppression due to frequency averaging, to -25 dB SNR. The incoherent estimator performance degraded below -20 dB. Both processors degraded when a sound speed error, $\delta c_{(\Delta h)}$ (introduced by a feature (Δh = 100) at 250 m depth in a water column of approximately 1000 m in depth), greater than .1 m/s was introduced. Positional errors of 1 m and 2 m for two of four hydrophones significantly degraded depth estimation in the coherent processor and no estimate was made with the incoherent scheme. The combined effects of small hydrophone positional errors combined with sound speed error clearly affected depth estimation. Neither of the two FUMFP estimators analyzed proved applicable for depth estimation for this experiment.

	additive noise*	SSP error**	hydrophone position** and SSP error
coherent	-25 dB	.1 m/s	0 m/s
incoherent	-20 dB	0 m/s	0 m/s

*** Includes potential frequency averaging gain (*M*=200)**
**** SSP error introduced by a 100 m feature at 250 m depth**
***** Adjust 2 of 4 vertical hydrophone positions by 1 and 2 m respectively**

Table 1. Tolerance results for four hydrophone FUMFP depth estimators.

b. Simulated Results - TDMSP

Although both TDMSP estimators appeared robust in response to additive noise and achieved accurate and unambiguous depth estimates in simulation, waveform correlation, did not provide accurate results when faced with sound speed errors. The magnitude matching estimator, however, provided an accurate depth estimate up to a sound speed error threshold of 3 m/s independently and to 2 m/s when combined with hydrophone position errors of 1 and 2 m for 2 of the 4 hydrophones. Clearly magnitude matching is the best choice of the four estimators.

	additive noise	SSP error*	hydrophone position** and SSP error
Waveform Correlation	-22 dB	.1 m/s	0 m/s
Magnitude Matching	-10 dB	3 m/s	2 m/s

*** SSP error introduced by a 100 m feature at 250 m depth**
**** Adjust 2 of 4 vertical hydrophone positions by 1 and 2 m respectively**

Table 2. Tolerance results for four hydrophone TDMSP depth estimators.

Unambiguous, yet inconsistent single hydrophone depth estimates were obtained utilizing magnitude matching of predicted to observed data recorded on Hydrophones 69, 77 and 78. The most probable cause for the difference between single hydrophone depth estimates (10.6 m, 11.8 m and 20.8 m) was analyzed by computer simulation. Hydrophone positional error is suspected as the cause.

2. Source Signal Waveform Reconstruction

a. Simulated Results

In the presence of simulated noise, the four hydrophone, frequency uncorrelated, least-squares estimator degraded noticeably at less than 5 dB of SNR. In light of introduced sound speed error, the ramp-up and ramp-down of the original signal

were successfully reconstructed but there was a significant deviation from the constant amplitude expected in simulations of $\delta c_{(\Delta h)}$ greater than .1 m/s.

b. Experimental Results and Recommended Direction

Unfortunately, neither the ramp-up / ramp-down slopes nor the constant amplitude of the assumed source signal waveform were reconstructed experimentally. The most probable reasons for this are the cumulative effects of background noise, sound speed error and hydrophone position inaccuracies. Evidence that the SNR threshold was exceeded is found in the experimentally obtained SNRs (approximately -5.3 dB for a detection range of 2326 m and -7.3 dB for a detection range of 3226 m) for the playback experiment. These values accurately reflect the SNRs experienced by the 3 hydrophones used in reconstruction. In order to properly validate this technique, a playback experiment would require a higher SL transmission.

There is a potential to achieve a better tolerance or lower SNR for source signal waveform reconstruction with this estimator by incorporating *a priori* or known parameters. Because frequency bandwidth, phase modulation and signal duration can be revealed with spectrograms, these *a priori* constraints could be included in future work. Source level estimates will remain a challenge, however, due to the lack of hydrophone sensitivity described in Hager (2008). Without an accurate conversion to μ Pa, source level (SL) cannot be estimated.

IV. CONCLUSIONS

Four primary goals were established for this dissertation; 1. Project a controlled and "representative" series of Odontocete vocalizations for digital recording and analysis while over the U.S. Navy SCORE Underwater Acoustic Range, 2. Obtain statistical measures of detection performance for extrapolation of detection range estimates with SL variability, 3. Test and refine *collective* three dimensional localization schemes through simulation and data-model comparisons of candidate methods and 4. Utilize inverse acoustic techniques for source signal waveform reconstruction. This closing section of the dissertation will address observations, challenges realized, and results from each of the 4 goals.

The playback experiment encountered two limitations, AGC adjustments on recorded hydrophone data and background clutter. The fixed AGC decreases amplitude when the received levels are too high and seriously hinders many aspects of this study, specifically SL calculations and source signal waveform reconstruction. The discussion of background clutter is two-fold. The first is inherent with the playback experiment itself while the second involves the presence of background anthropogenic noise. Playback clutter occurred as a result of "actual" vocalizations correlating with detector kernels rather than the transmitted signal while anthropogenic noise, that is, a fathometer, ship's sonar, etc., present a challenge if the signal was similar. It is the authors' opinion that the bulk of "in band" energy is of marine mammal origin.

As stated, the playback clutter induces a masking of the correlator or energy detector output intentionally reserved for the transmitted signal. To put it bluntly - the animals refused to remain quiet during transmission and often engaged in an interrogation / response dialogue with the J-9 sound source. A striking observation in the data revealed that an animal would mimic the transmitted signal almost perfectly in frequency versus time slope, often at a higher SL.

Statistical analysis of playback signals revealed valuable relationships for detection algorithms. Detection ranges to assure at least a 95% probability of detection and .01% false alarm rate were found to be 1600 m (energy detector) and 5100 m

(correlator) in the presence of background clutter. These experimental detection ranges were associated with a one second, downsweep, FM signal transmitted from 20 -10 kHz (SL= 135 dB re 1 μPa @ 1m). The signal was transmitted at a depth of approximately 15 meters.

Extrapolation of detection range estimates in a variable SL environment was accomplished using empirically derived SNR / detection ranges and a TL model that incorporated bottom, surface, and absorption losses. A 600 m detection range increase per 3 dB SL increase ratio was extracted. Most notably, a 3 dB increase in SL from that transmitted in this experiment resulted in nearly a 100% detection area coverage that assured a p(D) of 95% and p(FA) of .01% for the seven bottom hydrophones hexagonal pattern prevalent throughout the range.

Although not a limitation of this study, the band-pass nature of the bottom hydrophones will prove a challenge for future work at the Range. This prevented full exploitation of the previously documented and broadband nature of Odontocete vocalizations. Although the available band (8- 40 kHz consists of the low and high end frequency "roll offs" for bottom hydrophone detection) does contain portions of clicks and is well populated with whistles, the full frequency regime of vocalizations cannot be investigated. Additionally, the array is unable to record Mysticeti vocalizations, which are well known to occur below 8 kHz. Given the migration through and population of Gray whales and Blue whales in the immediate vicinity, the filtering represents a significant limitation.

The remaining two goals for this study, outlined in Section II, met with challenges as well. Horizontal localization was easily accomplished using time-difference-of-arrival processing of raw hydrophone data. Proven successful in previous studies, this method was extremely accurate and appears functional for use in automated localization systems.

TDMSP magnitude matching proved to be the best estimator of the four investigated, specifically in response to sound speed error, $\delta c_{(\Delta h)}$ (introduced by a 100 m feature at 250 m of water column depth) and hydrophone positional errors of 1 and 2 m for two of four hydrophones. Unambiguous, yet inconsistent, single hydrophone depth

estimates were obtained experimentally utilizing magnitude matching of predicted to observed data recorded on Hydrophones 69, 77 and 78. The difference between single hydrophone depth estimates (10.6 m, 11.8 m and 20.8 m) revealed a potential hydrophone positional error.

In the presence of simulated noise, the four hydrophone, frequency uncorrelated, least-squares estimator degraded noticeably with SNRs less than 5 dB. In light of introduced sound speed error, the ramp-up and ramp-down of the complex envelope of the assumed source signal were successfully reconstructed but there was a significant deviation from the constant amplitude, specifically when a sound speed error greater than .1 m/s was introduced.

Unfortunately, neither the ramp-up / ramp-down slopes nor the constant amplitude, characteristic of the assumed source signal waveform were reconstructed experimentally. The most probable reasons for this are the cumulative effects of additive noise, sound speed error and hydrophone position inaccuracies. Additionally, the playback transmission SL was too low. Experimentally obtained SNRs (approximately -5.3 dB for a detection range of 2326 m and -7.3 dB for a detection range of 3226 m) accurately reflect the SNRs experienced by the 3 hydrophones used in reconstruction. In order to properly validate this technique, a playback experiment would require a higher SL transmission.

A shortcoming of this study is the lack of hydrophone sensitivity. Without an accurate conversion to μPa, SL can not be estimated. There is a potential, however, to successfully reconstruct amplitude modulation. Given the parameters of frequency bandwidth, signal duration, and phase modulation (revealed in spectrograms) as *a priori* information, constraints could be applied to the least-squares estimator to achieve a successful reconstruction of the complex envelope magnitude in future studies.

THIS PAGE INTENTIONALLY LEFT BLANK

LIST OF REFERENCES

Abawi, A. T., Porter, M. B., Siderius, M., Hildebrand, J., Wiggins, S., "Model-based localization and tracking of marine mammals," J. Acoust. Soc. Am. 115 (5):2519(A) (2004).

Au, W. W. L, *The Sonar of Dolphins*, Springer-Verlag New York, Inc. (1993).

Au, W. W. L., Nachtigall, P. E., Pawloski, J. L., "Acoustic effects of the ATOC signal (75 Hz, 195 dB) on dolphins and whales," J. Acoust. Soc. Am. 101 (5):2973:2976 (1997).

Au, W. W. L., Herzing, D. L., "Echolocation signals of wild Atlantic spotted dolphin (*Stenella frontalis*)," J. Acoust. Soc. Am. 113 (1):598:604 (2003).

Au, W. W. L., Ford, J. K. B., Horne, J. K., Newman-Allman, K. A., "Echolocation signals of free-ranging killer whales (*Orcinus orca*) and modeling of foraging for Chinook salmon (*Oncorhynchus tshawytscha*)," J. Acoust. Soc. Am. 115 (2):901:909 (2004).

Ball, K. R., Buck, J. R., "Localization of dolphin whistles through frequency domain beamforming using a narrow aperture audio/video array," J. Acoust. Soc. Am. 113 (4):2307(A) (2003).

Bazua-Duran, C., Au, W. W. L., "The whistles of Hawaiian spinner dolphins," J. Acoust. Soc. Am. 112 (6):3064:3072 (2002).

Berggren, P., Wade, P. R., CARLSTRÖM, J., Read, A. J., "Potential limits to anthropogenic mortality for harbour porpoises in the Baltic region," **Biological Conservation**, 103:313-322 (2002).

Chiu, C.-S., Collins, C.A., Hager, C.A., Miller, C.W., Moore, T.C., Rocheleau, M.R., Lashkari, C., and Hayes, S., "A Feasibility Study of Monitoring Blue Whales Using the Pt Sur Ocean Acoustic Observatory," 134th Meeting of the Acoustical Society of America, San Diego, CA, 1-5 December 1997.

Chiu, C.-S., Miller, C.W., Moore, T.C., Collins, C.A., "Auto-detection and censusing of blue whale vocalizations along the central California Coast using a bottom-lying Hydrophone array," Proceedings of the Oceanology International '99 Pacific Rim Conference, 435-440 (1999).

Chiu, C.-S., Miller, C. W., Moore, T. C. , Collins, C. A., "Detection and Censusing of Blue Whale Vocalizations Along the Central California Coast Using a Decommissioned SOSUS Receiver," (Unclassified) JUA(USN), 2003 (S).

Chiu, C.-S., and Miller, C. W., "Whale monitoring," Chapter 17 in Sounds in the Sea: From Ocean Acoustics to Acoustical Oceanography, H. Medwin ed., Cambridge University Press. (2005).

Clark, C.W., Ellison, W.T., Beeman, K., "Acoustic tracking and distribution of migrating bowhead whales, *Balaena mysticetus*, off Point Barrow, Alaska in the spring of 1984," Rep. Int. Whal. Commn. 36:502 (1986).

Clark, C.W., Ellison, W.T. and Beeman, K., "Acoustic tracking of migrating bowhead whales," Oceans 86, IEEE Oceanic Eng. Soc., New York. 341:346 (1986).

Clark, C.W. 1994, " Basic understandings of whale bioacoustics: Potential impacts of man-made sounds from oceanographic research," J. Acoust. Soc of Am., 96 (5-2) 3269(A) (1994).

Clark, C.W. and D.K. Mellinger. "Application of Navy IUSS for whale research" J. Acoust. Soc. Am. 96 (5-2) 3315(A). (1994).

Clark, C.W., "Application of US Navy underwater Hydrophone arrays for scientific research on whales," Annex M (Matters Arising out of a Discussion of Blue Whales), Rep. int. Whal. Commn. 45: 210:212 (1995).

Clark, C.W., "Update on the Application of US Navy Underwater Hydrophone arrays for Scientific Research on Whales" Working Paper SCWP14 presented during the IWC Scientific Committee, Dublin, Ireland, May 1995. (1995).

Clark, C.W., An overview of the ATOC-Marine Mammal Research Program (ATOC-MMRP). Abstract. Eleventh Biennial Conference on the Biology of Marine Mammals, December 1995, Orlando, Fl. (1995).

Clark, C.W., and Charif, R.A. "Acoustic monitoring of large whales to the west of Britain and Ireland using bottom-mounted Hydrophone arrays, October 1996-September 1997," Joint Nature Conservation Committee (Aberdeen, Scotland) Report No. 281. (1998).

Clark, C.W., Ellison, W. T., "Calibration and comparison of the acoustic location methods used during the spring migration of the bowhead whale, *Balaena mysticetus*, off Pt. Barrow, Alaska, 1984-1993." J. Acoust. Soc of Am., 107(6) 3509:3517 (2000).

Croll, D. A., Clark, C. W., Calambokidis, J., Ellison, W. T., Tershy, B. R., "Effect of Anthropogenic Low-frequency Noise on the Foraging Ecology of Balaenoptera Whales" Animal Conservation Vol 4, 13:27 (2001).

Daziens, J. M., "Assessing the Performance of Omni-directional Receivers for Passive Acoustic Detection of Vocalizing Odontocetes." Naval Postgraduate School M.S. Thesis. (2004).

Dyer, I., "Statistics of Sound Propagation in the Ocean," J. Acoust. Soc. Am. 48(2) 337:345 (1970).

Finneran, J. J., Schlundt, C. E., Dear, R., Carder, D. A., Ridgway, S. H., "Temporary shift in masked hearing thresholds in Odontocetes after exposure to single underwater impulses from a seismic water gun," J. Acoust. Soc. Am. 111 (6):2929:2940 (2002).

Finneran, J. J., Carder, D. A., Ridgway, S. H., "Low-frequency acoustic pressure, velocity, and intensity thresholds in a bottlenose dolphin (*Tursiops truncatus*) and white whale (*Delhinapterus leucas*)," J. Acoust. Soc. Am. 111 (1):447:456 (2002).

Finnette, S., Mignerey, P. C., Smith, J. F., "Broadband source signature extraction using a vertical array," J. Acoust. Soc. Am, 94:309:318. (1993).

Frankel, A. S., and Clark, C. W., "Results of low-frequency m-sequence noise playbacks to humpback whales in Hawai'i," Can. J. Zool. 76: 521:535 (1998).

Frankel, A. S., and Clark, C. W. " Behavioral responses of humpback whales (*Megaptera novaeangliae*) to full-scale ATOC signals" J. Acoust. Soc. Am, 108(4), 1930:1937 (2000).

Frantzis, A., Goold, J. C., Skarsoulis, E. K., Taroudakis, M. I., Kandia, V., "Clicks from Cuvier's beaked whales, *Ziphius cavirostris* (L)," J. Acoust. Soc. Am. 112 (1):34:37 (2002).

Frietag, L. E., Tyack, P. L., " Passive acoustic localization of the Atlantic bottlenose dolphin using whistles and echolocation clicks," J. Acoust. Soc. Am. 94 (4):2197:2205 (1993).

Garcia, J. F., "Assessing the Performance of Omni-directional Receivers for Passive Acoustic Detection of Vocalizing Odontocetes: Initial Analysis." Naval Postgraduate School M.S. Thesis. (2002).

Hager, C. A., "Modeling the Performance of the Pt Sur Hydrophone Array in Localizing Blue Whales," Naval Postgraduate School M.S. Thesis. (1997).

Hager, C. A., "Assessment of the Performance of the Near-Bottom Hydrophones of the U.S. Navy Southern California Offshore Range in Detecting, Localizing and Reconstructing 10-20 kHz Odontocete Whistles," Naval Postgraduate School Ph.D. Dissertation. (2008).

Herman, L. M., Tavolga, W. N., "The communications systems of cetaceans," in *Cetacean Behavior: Mechanisms and Function*, Wiley-Interscience, New York, 149:209 (1980).

Howarth, E. S., Defran, R. H., "Nocturnal location and activity of Pacific coast bottlenose dolphins (*Tursiops truncatus*) determined by a sonobuoy array" J. Acoust. Soc. Am. 111 (5):2371(A) (2002).

Howarth, E. S., "Nocturnal distribution and movement of Pacific coast bottlenose dolphins (*Tursiops truncatus*) determined by acoustic localization. M.S. Thesis, San Diego State University, San Diego, Ca. (2003).

Janik, V. M., Van Parijs, S. M., Thompson, P. M., "A two-dimensional acoustic localization system for marine mammals," Marine Mammal Science 16, 437:447 (2000).

Janik, V.M., Source levels and the estimated active space of bottlenose dolphin (*Tursiops truncates*) whistles in the Moray Firth, Scotland. Journal of Comparative Physiology 186:673-680 (2000).

Jones, R. M., Riley, J. P., Georges, T. M., "*HARPO: A Versatile Three-Dimensional Hamiltonian Ray Tracing Program for Acoustic Waves in an Ocean with Irregular Bottom*," Wave Propagation Laboratory, National Oceanic and Atmospheric Administration, Boulder, CO, 457 pp. (1986).

Kumar, A., Miller, C. W., Chiu, C. S., "1998-99 blue whale call abundance off the central California coast using a bottom mounted Hydrophone.," J. Acoust. Soc. Am., 112 (5), 2399 (A) (2002).

Madsen, P. T., Carder, D. A., Au, W. W. L., Nachtigall, P. E., Mohl, B., Ridgway, S. H., "Sound production in neonate sperm whales (L)," J. Acoust. Soc. Am. 113 (6):2988:2991 (2003).

Mellinger, D. K., Clark, C. W., "Recognizing transient low-frequency whale sounds by spectrogram correlation," J. Acoust. Soc. Am., 107(6) 3518:3529. (2000).

Mignerey, P. C., Finette, S., "Multichannel deconvolution of an acoustic transient in an oceanic waveguide," J. Acoust. Soc. Am, 92 351:364. (1992).

Mitchell, S., Bower, J., "Localization of animal calls via hyperbolic methods," J. Acoust. Soc. Am. 97:3352:3353 (1995).

Mohl, B., Wahlberg, M., Madsen, P. T., Miller, L. A., Surlykke, A., "Sperm whale clicks: Directionality and source level revisited," J. Acoust. Soc. Am. 107 (1):638:648 (1997).

Mohl, B., Wahlberg, M., Madsen, P. T., Heerfordt, A., Lund, A., "The monopulsed nature of sperm whale clicks," J. Acoust. Soc. Am. 114 (2):1143:1154 (2003).

Moore, T.C., "Estimation of the Source Signal Characteristics and Variability of Blue Whale Calls Using a Towed Array," Thesis (MS in Meteorology and Physical Oceanography), Naval Postgraduate School. (1999).

Moore, S E. and Clark, J. T. " Potential impact of offshore human activities on gray whales (*Eschrichtius robustus*)," Journal of Cetacean Research and Management 4(1):19-25 (2002).

Nachtigall, P. E., Pawloski, J. L., Au, W. W. L., "Temporary threshold shifts and recovery following noise exposure in the Atlantic bottle nosed dolphin (*Tursiops truncatus*)," J. Acoust. Soc. Am. 113 (6):3425:3429 (2003).

Nishimura, Clyde E., Conlon, D. M., "IUSS Dual Use: Monitoring whales and earthquakes using SOSUS" Marine Technology Society Journal, vol. 27, no. 4, 13:21 (1994).

Philips, J. D., Nachtigall, P. E., Au, W. W. L., Pawloski, J. L., Roitblat, H. L., "Echolocation in the Risso's dolphin, *Grampus griseus*," J. Acoust. Soc. Am. 113 (1):605:616 (2003).

Rasmussen, M. H., Miller, L. A., Au, W. W. L., " Source levels of clicks from free-ranging white-beaked dolphins (*Lagenorhynchus albirostris* Gray 1846) recorded in Icelandic waters," J. Acoust. Soc. Am. 111 (2):1122:1125 (2002).

Richardson, W. J., Greene, C. .R., Malme, C. I., Thomson, D. H., *Marine Mammals and noise*. San Diego, CA: Academic Press. (1995).

Schlundt, C. E., "Temporary shift in masked hearing thresholds of bottlenose dolphins, *Tursiops truncates*, and white whales, *Delphinapterus leucas*, after exposure to intense tones," J. Acoust. Soc. Am. 107 (6):3496:3508 (2000).

Stafford, K. M., Fox, C. G., Clark, D. S., "Long-range acoustic detection and localization of blue whale calls in the northeast Pacific Ocean," J. Acoust. Soc. Am. 104 3616:3625 (1998).

Thode, A. M., Norris, T., Barlow, J., "Rapid estimation of dolphin whistle bearings using a sparse towed Hydrophone array," J. Acoust. Soc. Am. 106 (4):2188(A) (1999).

Thode, A., "Frequency beamforming of dolphin whistles using a sparse three-element Hydrophone towed array," J. Acoust. Soc. Am., 107 (6):3581-3584 (2000).

Thode, A. M., Howarth, E., Martinez, A., Stamates, J., "Automated two dimensional passive tracking of free-ranging dolphins using two towed arrays and frequency-domain beamforming," J. Acoust. Soc. Am. 112 (5):2399(A) (2002).

Thode, A., "Tracking sperm whale (*Physeter macrocehaplus*) dive profiles using a towed passive acoustic array," J. Acoust. Soc. Am. 116 (1):245:253 (2004).

Thomsen, F., Franck, D., Ford, J. K. B., "Characteristics of whistles from the acoustic repertoire of resident killer whales (*Orcinus orca*) off Vancouver Island, British Columbia," J. Acoust. Soc. Am. 109 (3):1240:1246 (2001).

Tiemann, C. O., Porter, M. B., Frazer, L. N., "Automated model-based localization of marine mammals near Hawaii," J. Acoust. Soc. Am. 110 (5):2717(A) (2001).

Tiemann, C. O., Porter, M. B., Hildebrand, J., "Model-based tracking of marine mammals near California using seismometers," J. Acoust. Soc. Am. 112 (5):2262(A) (2002).

Tiemann, C. O., Porter, M. B., "A comparison of model-based and hyperbolic localization techniques as applied to marine mammal calls," J. Acoust. Soc. Am. 114 (4):2406(A) (2003).

Tiemann, C. O., Porter, M. B., Frazer, L. N., "Localization of marine mammals near Hawaii using an acoustic propagation model," J. Acoust. Soc. Am. 115 (6):2834:2843 (2004).

Tolstoy, A., *Matched Field Processing for Underwater Acoustics*, World Scientific Publishing Co, River Edge, NJ. (1993).

Watkins, W.A., and W.E. Schevill, "Listening to Hawaiian spinner porpoises (*Stenella* cf. *longirostris*) with a three-dimensional Hydrophone array". Journal of Mammalogy 55:319-328 (1974).

Wiggins, S. M., McDonald, M. A., Munger, L., Hildebrand, J. A. and Moore, S. E., Waveguide propagation allows range estimates for North Pacific right whales in the Bering Sea, Canadian Acoustics, 32(2), 146:154 (2004).

INITIAL DISTRIBUTION LIST

1. Defense Technical Information Center
   Ft. Belvoir, Virginia

2. Dudley Knox Library
   Naval Postgraduate School
   Monterey, California

3. Dr. Ching-Sang Chiu
   Office of Naval Research
   Arlington, Virginia

4. Dr. Lawrence Ziomek
   Naval Postgraduate School
   Monterey, California

5. CDR Ben Reeder, USN
   Naval Postgraduate School
   Monterey, California

6. Dr. Jim Harvey
   Moss Landing Marine Laboratories
   Monterey, California

7. Chris Miller
   Naval Postgraduate School
   Monterey, California

8. CDR Carl Hager, USN
   Department of Oceanography
   United States Naval Academy

9. CDR John Joseph, USN (ret)
   Department of Oceanography
   United States Naval Academy